

**POLITECNICO DI MILANO**

**School Of Industrial And Information Engineering**

**Master Of Science In Biomedical Engineering**



**Hydrophobins As Effective Biosurfactants For Aqueous  
Dispersions Of Carbon Nanomaterials**

**SUPERVISOR : Prof. Pierangelo Metrangolo**

**CO-SUPERVISOR : Dr. Valentina Dichiarante**

**Master Thesis Of:**

**Paul Pradeep John Peter**

**ID 893589**

**Academic Year 2018 – 2019**

# ACKNOWLEDGEMENTS

Finally, a journey going to end with the start of a new one. First and foremost I would like to express my sincere gratitude to Prof. Pierangelo Metrangolo for giving this wonderful opportunity to carry out master thesis In his laboratory (SUPRABIONANO LAB) and the trust in giving me this thesis project. A huge thanks to Dr. Valentina Dichiarante who was guiding me throughout the project and spending the valuable time with me despite her busy schedule. Through this short period of time in the lab , I have learnt many things which will be valued throughout my life. I am really sorry if some of my action made you angry. I will surely prove to be the best in the future.

I would like to thank Italian government (MAECI) for giving me the scholarship to study master of science in biomedical engineering at Politecnico di Milano, Italy. I would like to show my gratitude to all the professors associated with me throughout the coursework without them completing the degree would have been not possible.

My Joy has no bounds in expressing my cordial gratitude to my friend Geetha Balsubramani, Her keen interest and encouragement were a great help throughout the course of this degree and research.

In addition, I would like to thank my parents for their wise counsel and sympathetic ear. You are always there for me. Finally, there are my friends, who were of great support in deliberating over my problems and findings, as well as providing happy distraction to rest my mind outside of my studies and problems.

Thank you all once again !!!

# ABSTRACT

In the pressing need of greener and more sustainable alternatives to replace synthetic surfactants, a valuable strategy is offered by the use of amphiphiles of biological origin. Among them, fungal Hydrophobins already proved to be highly effective dispersing agents for a wide range of hydrophobic materials. These low molecular weight amphiphilic proteins owe their extremely high surface activity and film-forming ability to the presence on their surface of a discrete portion composed of hydrophobic aminoacids, called 'hydrophobic patch'. This structural feature drives the spontaneous self-assembly of HFBs into strong and elastic films at both air/water and hydrophobic/hydrophilic interfaces, promoting their successful exploitation as novel biosurfactants, coating agents, and surface modifiers.

Carbon nanomaterials have gained huge research interest in recent days, due to their availability and cost-effectiveness. They have been studied intensively in various fields, such as biology, medicine, chemistry and mechanics, due to their properties, i.e. good electrical conductivity, high surface area, linear geometry, good mechanical strength, good optical properties and low cytotoxicity. Unfortunately, carbon nanomaterials are highly insoluble in aqueous media, which makes it very difficult for many applications.

This thesis aims to demonstrate the possibility to exploit the surfactant properties of a hydrophobin (HFBII) for obtaining stable aqueous dispersions of carbon blacks, both fluorinated and not. Dynamic Light Scattering (DLS), Fourier Transform Infrared spectroscopy (ATR-FTIR), Nuclear Magnetic Resonance (NMR) and Transmission Electron Microscopy (TEM) were used to characterize the resulting samples and to confirm the ability of such protein to form a film around carbon blacks particles and to disperse them in water. Stable aqueous dispersions of these carbon nanomaterials may potentially open a door to a new era of applications in the field of science and engineering, that are more environment-friendly and biocompatible.

***Keywords : Hydrophobin, Biosurfactant, Carbon nanomaterials, Water dispersibility, Surface modification.***



# CONTENTS

ACKNOWLEDGEMENTS .....	2
ABSTRACT .....	3
LIST OF FIGURES .....	7
1. INTRODUCTION .....	9
1.1 CLASS II HYDROPHOBINS (HFBI, HFBII).....	12
1.2 HYDROPHOBINS AS SURFACTANTS.....	14
1.3 INTRODUCTION TO CARBON NANOMATERIALS .....	16
1.3.1 PROPERTIES .....	18
1.3.2 APPLICATIONS .....	19
1.4 INTRODUCTION TO CARBON BLACKS AND THEIR FLUORINATED ANALOGUES .....	20
1.5 HYDROPHOBINS AS DISPERSIVE AGENTS FOR CARBON MATERIALS .....	23
1.6 OBJECTIVE OF THIS PROJECT .....	25
2. MATERIALS AND METHODS .....	26
2.1 MATERIALS.....	26
2.2 METHODS .....	26
2.2.1 DYNAMIC LIGHT SCATTERING .....	27
2.2.2 ATR-FTIR .....	29
2.2.3 TEM (Transmission Electron Microscopy).....	32
2.2.4 NMR (Nuclear Magnetic Resonance).....	35
3. RESULTS AND DISCUSSION.....	37
3.1 DISPERSION OF CARBON BLACKS (CB) AND FLUORINATED CARBON BLACKS (FCB) IN ORGANIC SOLVENTS.....	37
3.1.1 TEM IMAGES OF THE STARTING CARBON BLACKS AND FLUORINATED CARBON BLACKS IN ORGANIC SOLVENTS .....	38
3.2. DISPERSION OF STARTING CBS IN AQUEOUS HYDROPHOBIN (HFBII) SOLUTION .....	39
3.2.1 TEM IMAGES OF THE STARTING CARBON BLACKS IN HFBII-MilliQ WATER .....	40
3.2.2 ATR-FTIR ANALYSIS OF THE STARTING CARBON BLACKS IN HFBII- MilliQ WATER .....	42

3.2.3 DLS ANALYSIS OF THE STARTING CARBON BLACKS IN HFBII-MilliQ WATER .....	43
3.3. DISPERSION OF FLUORINATED CARBON BLACKS (FCB) IN HYDROPHOBIN (HFBII) SOLUTION .....	44
3.3.1 TEM IMAGES OF FLUORINATED CARBON BLACKS IN HFBII-MilliQ WATER .....	44
3.3.2 ATR-FTIR ANALYSIS OF FLUORINATED CARBON BLACKS IN HFBII-MilliQ WATER .....	47
3.3.3 DLS ANALYSIS OF FLUORINATED CARBON BLACKS IN HFBII-MilliQ WATER .....	48
3.3.4 <sup>19</sup> F-NMR ANALYSIS OF FLUORINATED CARBON BLACKS IN HFBII-MilliQ WATER .....	49
4. CONCLUSIONS AND FUTURE PERSPECTIVES.....	51
5. REFERENCES .....	54

# LIST OF FIGURES

Figure 1 Fungal Hydrophobin an overview.....	11
Figure 2 Structure of T.resei Hydrophobin.....	12
Figure 3 X-ray crystal structure of HFBII.....	13
Figure 4 The schematics of the representative carbon-based nanomaterials.....	17
Figure 5 Dynamic Light Scattering instrument setup.....	28
Figure 6 Schematic diagram of a horizontal ATR sampling.....	30
Figure 7 Thermo Fisher Nicolet iS50 FTIR Spectrometer.....	31
Figure 8 Simplified diagram of a transmission electron microscope.....	33
Figure 9 NMR spin- $\frac{1}{2}$ nuclei model.....	35
Figure 10 Dispersion of starting carbon blacks in Ethanol.....	37
Figure 11 Dispersion of Fluorinated carbon blacks in Ethanol.....	37
Figure 12 TEM image of non-fluorinated carbon blacks in an organic solvent.....	38
Figure 13 TEM image of fluorinated Carbon blacks in an organic solvent.....	38
Figure 14 Dispersion of carbon blacks in HFBII-MilliQ water.....	39
Figure 15 TEM images of CBs in HFBII-MilliQ prepared using US bath for 30 minutes.....	40
Figure 16 TEM images of CBs in HFBII-MilliQ prepared using tip sonication for 5 minutes.....	40
Figure 17 ATR-FTIR spectra of Crude carbon black powder, HFBII in MilliQ and the sample (CB+HFBII).....	42
Figure 18 DLS comparison between carbon blacks suspended in ethanol and in HFBII-MilliQ: a) Correlation function at 90° b) Intensity-weighted average size distribution at 90° obtained by CONTIN fit.....	43
Figure 19 Dispersion of fluorinated carbon blacks in HFBII-MilliQ water.....	44
Figure 20 TEM images of fluorinated carbon blacks (FCB) with HFBII in MilliQ water obtained after 30 min of ultrasound bath sonication.....	45
Figure 21 TEM images of FCBs with HFBII in MilliQ water obtained after tip sonication for 5 mins.....	46

Figure 22 ATR-FTIR spectra of Fluorinated carbon blacks powder, HFBII in MilliQ and the sample (FCB+HFBII).....	47
Figure 23 DLS analysis of fluorinated carbon blacks in HFBII-MilliQ: a) Correlation functions at 90° b) Intensity-weighted average size distribution at 90° obtained with CONTIN fit.....	48
Figure 24 <sup>19</sup> F-NMR spectra (ref. 2,2,2-trifluoroethanol in D2O) FCB + HFBII – US bath 30’.....	49
Figure 25 <sup>19</sup> F-NMR spectra (ref. 2,2,2-trifluoroethanol in D2O) FCB + HFBII – Tip sonicator 5’ min.....	50
Figure 26 Hydrophobin prospects in the field of biosurfactants.....	52



# 1. INTRODUCTION

Hydrophobins are a group/family of low molecular weight amphiphilic proteins, generally between 7-15 kDa. Hydrophobins are non-toxic and environment-friendly proteins which are known for their peculiar surface properties [1]. They are known to form hydrophobic coatings on the surface of nano- or microparticles which are insoluble in water / aqueous media. The first Hydrophobin genes were found in a search for abundantly expressed genes during the development of *Schizophyllum commune* without then knowing the personality and nature of such proteins.

Fungi are heterotrophic terrestrial eukaryotes, showing two types of growth morphologies: unicellular yeast and multicellular filamentous forms. Yeasts are hydrophilic and they lack Hydrophobins. The vegetative hyphae of filamentous fungi growing on moist environments are also hydrophilic and do not show the presence of rodlets on their surface. In contrast, the aerial hyphae and the asexual spores (conidia) are hydrophobic, due to the presence of Hydrophobins [2]. The functions of Hydrophobins are related to their high surfactant activity, which results from their self-assembly at hydrophilic–hydrophobic interfaces to form an amphipathic monolayer. The Hydrophobin layer reduces the surface tension of the medium or the substratum in/on which fungi grow, allowing them to breach the air–water interface or preventing water-logging while maintaining permeability to gaseous exchange. Spores produced on the aerial structures of filamentous fungi are covered by a Hydrophobin rodlet layer that renders the conidial surface hydrophobic and wet-resistant, thus facilitating spore-dispersal in the air. The rodlet-forming Hydrophobins are essential for these fungi to complete their biological cycle. In many “wet” fungi (e.g., *Conidiobolus obscurus*), the rodlet-layer is covered by a mucilaginous extracellular matrix that helps the conidia to bind to the substrate, and once the spores are bound to the host, the rodlet-layer is unmasked for better resistance to the environment. Hydrophobins show very little sequence conservation in general, apart from the idiosyncratic pattern of eight Cys residues implicated in the formation of four disulfide bridges (Cys1–Cys6, Cys2–Cys5, Cys3–Cys4, Cys7–Cys8) [2]. They are small (~100 amino acids) cysteine-rich proteins that are expressed only by filamentous fungi. HFBs usually comprise of about 100 amino acids and

dependably contain four disulfide bridges in the protein center, which give astounding security to their structure [3]. Their remarkable amphiphilic conduct is due to the presence on their surface of a discrete part completely made from amino acids with hydrophobic side chains, the alleged 'hydrophobic patch'. This structural ability drives the unconstrained self-assembly of HFBs into solid and versatile film at both air/water and hydrophobic/hydrophilic interfaces, advancing their fruitful exploitation as novel biosurfactants, coating and adhesion agents, and as surface modifiers. Based on differences in surface and structural properties, they can be divided into two categories: class I and class II. Hydrophobins can self-assemble into a monolayer on hydrophilic/hydrophobic interfaces such as a water/air interface. Class I monolayer contains the same core structure as amyloid fibrils, and is positive to Congo red and thioflavin T. The monolayer formed by class I Hydrophobins has a highly ordered structure and can only be dissociated by concentrated trifluoroacetate or formic acid. Monolayer assembly involves large structural rearrangements with respect to the monomer [1]. The biological function of Hydrophobin is diverse and is strongly related to its strong surface activity. Hence, much of the attention to date has inevitably focused on investigating its surface adsorption properties and self-assembly at interfaces [3].

Class I Hydrophobins are small amphipathic proteins that self-assemble to form functional amyloid fibrils, known as rodlets, on the surface of fungal structures such as aerial hyphae and spores. The rodlets form a monolayer through lateral association and are highly robust; dissociation is only possible with certain concentrated acids. This monolayer is amphipathic, with the hydrophobic face as water-resistant as Teflon [13]. In class I, considerable variation is seen in the inter-Cys-spacing; these Hydrophobins assemble into highly insoluble polymeric monolayers composed of fibrillar structures known as rodlets [2]. The rodlets are extremely stable, can only be solubilized with harsh acid treatments, and the soluble forms can polymerize back into rodlets under appropriate conditions.

Despite the low sequence similarity, class I Hydrophobins from different fungal species could partially complement a *Magnaporthe grisea* class I Hydrophobin gene (MPG1) deletion mutant, suggesting that Hydrophobins constitute a closely related group of morphogenetic proteins. The sequence and the inter-Cys spacing are more conserved in class II; the monolayers formed by

class II Hydrophobins lack the fibrillar rodlet morphology and can be solubilized with organic solvents and detergents. Surface film at air-water interfaces are reported for both the class of Hydrophobins, with differences only in protein-protein interaction [3].

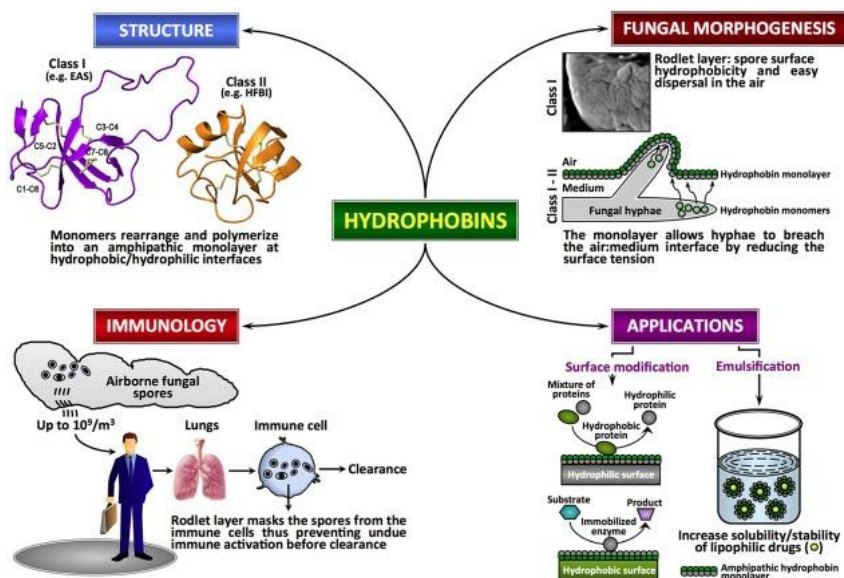


Figure 1 Fungal Hydrophobin an overview [ doi: 10.1371/journal. Pat. 1002700.g001] Copyright Bayry et al. [3]

Figure 1 shows the overview of fungal protein Hydrophobins. Fungal morphogenesis with its structure, immune adaptive capacity and application are shown as a scheme for understanding. The potential uses of Hydrophobins depend on their capacity to turn around the hydrophilic-hydrophobic character of a surface or potentially their surfactant limit [3]. A few biotechnological utilizations of Hydrophobins have been proposed. However, the vast scale uses of Hydrophobins may be hard to actualize because of the generation cost of recombinant proteins as well as the substantial scale prerequisites of the proteins. Interestingly, in the pharmaceutical or in the nanotechnology business, where the profits of venture are high, it is conceivable to imagine a potential advancement for these proteins [4].

## 1.1 CLASS II HYDROPHOBINS (HFBI, HFBII)

The filamentous fungi *Trichoderma Reesei* produces class II Hydrophobins (HFBI and HFBII). Class II Hydrophobins are soluble in aqueous dilutions of organic solvents, e.g. ethanol (60%) or surfactant such as hot sodium dodecyl sulfate (2% SDS). Class II monolayer lacks the rodlet morphology and is less stable [2]. Class II Hydrophobins have higher emulsifying activity and longer stabilizing period of oil droplets than class I Hydrophobins [4]. The structure of the *T. reesei* HFBII Hydrophobin shows an amphiphilic molecule with one hydrophilic and one hydrophobic part. Figure 2A shows a cartoon of the secondary structure elements in HFBII. There is a central  $\beta$  sheet structure that is formed by two  $\beta$  hairpins. The two loops of the hairpins form most of the hydrophobic patch. In Figure 2B, a space-filling model of the structure in

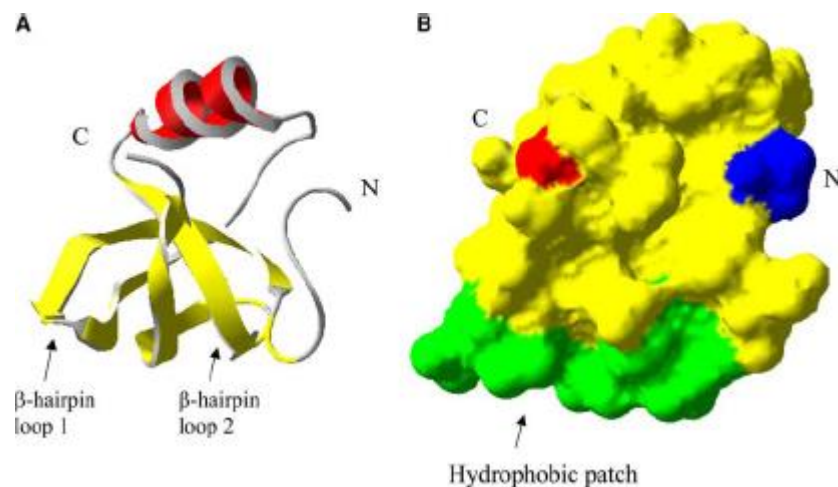


Figure 2 Structure of *T. reesei* Hydrophobin A) Cartoon of secondary structure of Hydrophobin B) Space filling model of structure Green- Hydrophobic patch, blue – N terminal, red – C terminal [9]

the same scale and orientation shows the hydrophobic patch in green, the rest of the surface in yellow, except for the N- and C-termini that are indicated in blue and red, respectively.

The coordinates for the structure are available from the protein data bank with the identification number 1R2M [9]. Analysis of the surface residues of HFBII reveals a large patch consisting of Hydrophobic aliphatic residues. This Hydrophobic patch is formed mainly by residues near the loop-regions of the two  $\beta$  hairpins. The surface is relatively flat and comprises about 12% of the

total surface area of the protein [2]. About half of the hydrophobic aliphatic residues of HFBII are located at the surface, forming this patch. In contrast, the hydrophobic residues in soluble proteins in general typically form hydrophobic cores that stabilize their folded structures. HFBII can be thought of as being turned inside-out in this respect because it exposes such a large fraction of its hydrophobic residues. To compensate for the destabilizing effect of the exposed hydrophobic residues, the structure is strongly stabilized by disulfide bonds [8]. Class II hydrophobins self-assemble into non-fibrillar films that can be dissociated by treatment with alcohol solutions and detergents [8]. These biocompatible, self-assembling, amphipathic films show promise for use in nanotechnology applications, including coating implanted medical devices, biosensors and cell growth surfaces [9–13]. An understanding of the molecular basis for hydrophobin self-assembly is required in order to control the morphology and properties of these protein layers. The soluble forms of the hydrophobins share a similar structural scaffold imposed by the network of disulfide bonds, while sequence diversity between family and class members is accommodated in diverse secondary structural elements and loop regions [14]. The hydrophobins have relatively large, exposed hydrophobic patches on the protein surface and display a clustering of surface charged residues that is likely to underpin the observed high surface activity of these proteins.

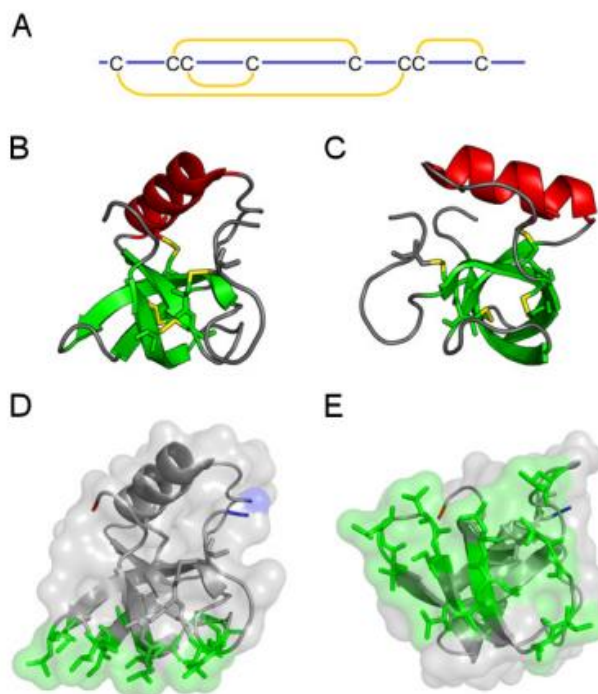


Figure 3 : X-ray crystal structure of HFBII

Figure 3. X-ray crystal structure of HFBII (PDB ID 1R2M) (Hakanp et al. 2004). (A) Cartoon of the conserved Cys residue pattern in the hydrophobin amino acid sequences. The disulfide bonding pattern is shown in yellow. (B and C) Cartoon of the protein backbone structure showing the  $\beta$ -barrel formed by two  $\beta$ -hairpins (green) and the connecting  $\alpha$ -helix (red). The disulfide bonds of Cys residues are shown in yellow. (D and E) Surface representation of HFBII in which the side chains of the conserved hydrophobic patch are shown and colored green. N- and C- termini are colored in blue and red, respectively. The hydrophobic patch is viewed from the side in panel (D) and from above in (E). The images were produced using PyMol

## 1.2 HYDROPHOBINS AS SURFACTANTS

Biosurfactants are of much current interest because of their properties relating to biosustainability and biodegradation. A wide range of different biosurfactants have been studied and include glycolipids, such as the rhamnolipids, sophorolipids, and mannosylerythritol lipids, lipopeptides and proteins, such as surfactin and Hydrophobins. Their novel adsorption and self-assembly properties lead to many interesting potential applications, and yet many of these aspects are poorly characterized or understood. Furthermore, many potential applications will involve mixtures with a range of surfactants and other proteins, and both the surface adsorption and self-assembly properties of such mixtures have not been extensively explored. Hydrophobins have been found as both efficient, non-toxic and environment friendly [5].

The self-assembly of the protein HFBII and its self-assembly with cationic, anionic, and nonionic surfactants hexadecyltrimethyl ammonium bromide, CTAB, sodium dodecyl sulfate (SDS), and hexaethylene monododecyl ether (C12E6), in aqueous solution have been studied by small-angle neutron scattering (SANS). HFBII self-assembles in solution into small globular aggregates, consistent with the formation of trimers or tetramers. Its self-assembly is not substantially affected by pH or by the presence of electrolytes. In the presence of CTAB, SDS, or C12E6, HFBII/surfactant complexes are formed. The structure of the HFBII/surfactant complexes has been identified using contrast variation and is in the form of HFBII molecules bound to the outer surface of globular surfactant micelles. The binding of HFBII decreases the

surfactant micelle aggregation number for increasing HFBII concentration in solution, and the number of Hydrophobin molecules bound/micelle increases [6].

Class II Hydrophobin HFBII from *Trichoderma reesei* was used as a surfactant to stabilize the oil/water interfaces in the continuous aqueous phase. Recently it was reported that Hydrophobins along with Nano Fibrillated cellulose increased the emulsion stability for encapsulation and release of BCS class II drugs (ibuprofen and ketoprofen). HFBs are nontoxic by themselves which is a prerequisite for pharmaceutical excipients. Additionally, a surface layer of HFB on the airborne fungal spores has been shown to prevent immune recognition. This is an attractive feature for materials in pharmaceutical applications. Class II *Trichoderma reesei* HFBs (e.g., HFBI, HFBII and HFBIII) are more water soluble than class I HFBs and can be easily dissolved at rather high concentrations in aqueous solutions.

The overall structure therefore resembles the structure of surfactants with one hydrophobic and one hydrophilic part. The amphiphilicity makes HFBs suitable surface coating materials for pure drug crystals as well as drug carrier materials. HFBs have been successfully used as surfactants, encapsulating agents for nutraceuticals and coatings for drug nanoparticles (NPs). HFBII coating on the surface of drug NPs has been shown to introduce mucoadhesive properties to drug NPs in the Gastro Intestinal Tract (GIT). For poorly water-soluble drugs, mucoadhesive formulations are beneficial for improving drug bioavailability due to the prolonged time at the site of drug absorption[7].

Recently NFC (Nano fibrillar cellulose) has been used in combination with HFBs to produce emulsions, stabilize drug Nano-crystals and to produce aerogel matrices for HFB coated drug NPs. It has been shown in previous studies that HFBs and NFC can be used successfully to stabilize o/w emulsions. Surface active HFB fusion proteins that contained cellulose-binding domains from cellulolytic enzymes were used. By combining the fusion protein HFBs and NFC emulsions that contained tightly packed thin NFC films at the oil/water interface were obtained. In this study *Trichoderma reesei* HFBII and NFC were used for the stabilization of pharmaceutical emulsions. Due to the interesting surface properties, low toxicity and good biocompatibility of both NFC and HFBII, these materials were selected to produce o/w emulsion formulations [6].

The emulsions were utilized for the embodiment and release of inadequately water solvent BCS II drugs (Biopharmaceutics Classification System II – High Permeability, Low Solubility) naproxen (NAP) and ibuprofen (IBU). HFBII was utilized as a surfactant to balance out the o/w interface of the emulsions, though NFC was added to change the thickness of the constant fluid stage.

The stabilization of fluoruous oil droplets in aqueous environment is a critical issue in the preparation of emulsified systems for biomedical applications and in emulsion polymerization technology. For this purpose, perfluorosulfonic acids (PFSAs) and perfluorocarboxylic acids (PFCAs), and their salts have been largely used as surfactants. However, huge concerns have been raised around their use, since many of them are persistent organic pollutants (POPs). Perfluorooctanesulfonic acid (PFOS) and perfluorooctanoic acid (PFOA) are of greater concern as they bio-accumulate in the food chain. As a result of which Hydrophobins are studied as alternative surfactants which are naturally occurring.

HFBs have been applied as foaming and antifouling agents, adhesion promoters, fatty oil/water emulsion stabilizers and enhancers, as well as in personal care and biomedical applications. A few studies have also shown that, thanks to their hydrophobic patch, HFBs possess the capability to assemble into films on solid fluorinated surfaces from aqueous solutions, despite the Omni repellency of such surfaces. In one recent case, HFB-stabilized perfluoroalkane/water emulsions have been used as templates for the growth of mineral shells by Boker and coworkers [18]. With the idea that HFBs are natural non-toxic compounds that may not only be well-suited to biomedical applications, but which may also represent a more sustainable alternative to synthetic fluoro-surfactants commonly employed e.g. in emulsion polymerization or in microfluidic systems, Roberto Milani et al decided to investigate systematically the behavior of Hydrophobins at the interface between aqueous and fluoruous phases[6].

### 1.3 INTRODUCTION TO CARBON NANOMATERIALS

Carbon materials have played important roles for human beings: charcoals as a heat source and as an adsorbent since prehistorical age, flaky natural graphite powder as pencil lead, soot in black ink for the development of communication techniques, graphite electrodes for steel



production, carbon blacks for reinforcing tires in order to develop the motorization, electric conductive carbon rods and carbon blacks for supporting the development of primary batteries, a compound of graphite with fluorine (graphite fluoride) for improving the performance of primary batteries, thin graphite flakes in membrane switches for making computers and control panels thinner and lighter, etc. In relation to global-warming problems, nuclear reactors are recognized to be important, which are constructed from high-density isotropic graphite blocks, having different roles as reflectors, moderators, etc. For the storage and efficient usage of sustainable energies, which are usually unstable, lithium-ion rechargeable batteries and electric double-layer capacitors are essential devices, in which carbon materials are used as electrodes and govern their performance: in the former, lithium intercalation/deintercalation into the galleries of the anode graphite is a fundamental electrochemical reaction and, in the latter, physical adsorption of electrolyte ions onto the surfaces of the electrodes of porous carbon is a fundamental electrochemical reaction. Nano-carbons developed recently, which are represented by carbon nanotubes, fullerenes, and graphene, are promoting the development of nanotechnology in various fields of science and engineering [9].

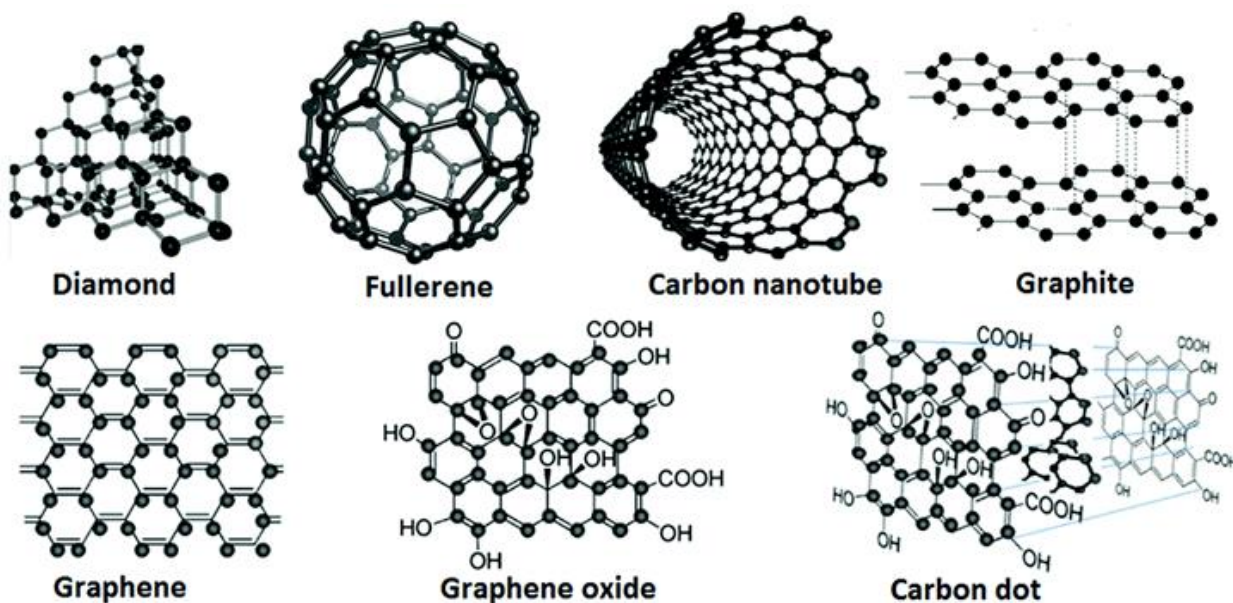


Figure 4 The schematics of the representative carbon-based nanomaterials [19] copyright from CD

Carbon materials are predominantly composed of carbon atoms, only one kind of element, but they have largely diverse structures and properties. Diamond has a three-dimensional structure and graphite has a two-dimensional nature, whereas carbon nanotubes are one-dimensional and buckminsterfullerene C<sub>60</sub> is quasi-zero-dimensional. Fullerenes behave as molecules, although other carbon materials do not. Graphite is an electric conductor and its conductivity is strongly enhanced by AsF<sub>5</sub> intercalation, higher than metallic copper, whereas diamond is completely insulating. Diamond is the hardest material is used for cutting tools, whereas graphite is so soft that it can be used as a lubricant.

Carbon nanotubes (CNTs) are allotropes of carbon with a cylindrical nanostructure, exhibiting many unique physical, mechanical and chemical properties which have drawn great attention in the past decade [10]. Owing to their well-known surface structure, outstanding electronic performance and biochemical stability, CNTs can serve as excellent substrates for the development of biosensors or as a modifier to promote electron transfer reactions between many biologically important species with the underlying electrode. For example, CNTs can be used as a reaction promoter in biosensors for the electrochemical detection of dopamine and hydroquinone. It has also been shown that CNTs could improve the direct electron transfer of some important biomolecules including cytochrome c, myoglobin and horseradish peroxidase (HRP). However, the insolubility of CNTs in all solvents can be a major drawback to their use in electrochemical sensors and biosensors. Functionalization of CNTs can improve their solubility and processability, giving the opportunity to develop new types of nanotube-based materials [11] [12].

### 1.3.1 PROPERTIES

Carbon nanoparticles have extraordinary electrical conductivity, heat conductivity, and mechanical properties. They are composed of pure carbon, therefore, exhibiting high stability, good conductivity, low toxicity, environmental friendliness. Since a large part of the human body consists of carbon, they are generally thought as biocompatible materials. The good electrical conductivity, high surface area, and linear geometry make their surface highly accessible Carbon-based nanomaterials also have strong anisotropic thermal conductivity. This

property allows the carbon-based nanomaterials being used in advanced computing electronics where the temperature of uncooled chips can reach over 100°C.

Carbon nanomaterials and its allotropes are not dispersible in water, where they aggregate together or settle down without forming a monodisperse solution. If the solubility or the dispersive ratio of carbon material is altered then it can be a beginning for the new era of application in the field of Biology, Chemistry, Physics and much more. Surfactants and emulsifiers are used continuously to achieve monodisperse solution. Hydrophobins can be used as surfactants to cover the surface of materials, converting them to be dispersive and useful for many applications.

### 1.3.2 Applications

#### *Drug and gene delivery*

The exploration of carbon-based nanomaterials in biomedical applications is at the early stages but has attracted tremendous attention. One hot topic is their application in drug and gene delivery. For example, some research studies have shown that CNTs can be bonded to a single strand of DNA and can then be successfully inserted into a cell. By functionalizing and chemically modifying the sidewall, CNTs can also be used as vascular stents and for neuron growth and regeneration. Applications in drug delivery is very common for carbon-based nanoparticles, especially for graphene-based nanoparticles. Their  $\pi$ -conjugated structure of six-atom rings of can be conceptually considered as a planar aromatic macromolecule. This unique structure offers a large loading capability to a variety of fluorescent probes and drugs [19][20]. The chemical modification of graphene can allow the conjugation with targeting ligands, and therefore the achievement of the targeted delivery of the drug. Both *in vitro* and *in vivo* studies have provided the evidence of the graphene for delivering anti-cancer drugs to the desired location of tumour cells, rather than the normal and healthy cells[20].

## *Bioimaging*

Carbon-based materials have been long investigated in many imaging applications. For example, fluorescence imaging (FL), two-photon FL, Raman imaging, magnetic resonance imaging (MRI), tomography (CT), photoacoustic imaging (PAI), computed positron emission tomography/single photon emission computed tomography (PET/SPECT), and multimodal imaging. Recently, a new form of carbon-based nanomaterials, carbon quantum dots, has attracted tremendous interests in its bioimaging applications. Since the original report in 2006, CQDs has been widely investigated for its fluorescent property. Like traditional QDs, CQDs possess size-dependent tunable emission and can be resistant to photobleaching, making it desired for as bioimaging agent [20]. Moreover, it also overcomes the severe toxicity of traditional QDs composed of heavy metals such as cadmium. Therefore, its bioimaging and biological labelling applications have been extensively examined in both cells and animal models.

## *Energy storage*

Due to the dwindling of fossil fuel resources, the implementation of practical alternative energy systems becomes extremely important. Fuel cells may be one of the most likely energy sources. Carbon-based nanomaterials have been widely investigated as the catalysts and key components of hydrogen storage systems. Due to their intrinsic characteristics, carbon-based materials are a desired material as electrodes in capacitors and batteries. CNTs have shown a high reversible capacity for use in lithium-ion batteries and also in a variety of fuel cell components. The high electrical conductivity also allows CNTs to be used in current collectors and gas diffusion layers. The high surface area and thermal conductivity make CNTs and graphene very useful as electrode catalyst supports in fuel cells.

## **1.4 INTRODUCTION TO CARBON BLACKS AND THEIR FLUORINATED ANALOGUES**

Carbon nanoparticles, including carbon nanotubes (CNTs), carbon blacks, graphene carbon, nanofibers (CNFs) and buckyballs (fullerene) are of great interest worldwide for many industrial applications because of their excellent mechanical, electrical, thermal and optical properties.

The major industrial applications of the carbon nanoparticles are rubber and tire toughening in nanocomposite forms, coating, corrosion protections, batteries, sensors, laser printer ink, charging and discharging, heat sink, solar energy and storage, electronics, and so on. A number of physical, and chemical techniques have been developed and used for the fabrications of carbon nanoparticulates in various size, shape and morphologies for different industrial applications and scientific.

The use of nanoparticles such as metal oxides, carbon nanotubes, and fullerenes (e.g.,  $C_{60}$ ) has become popular in a wide range of commercial products such as photocatalysts, sunscreen, cosmetics, pigments, and semiconductors. After use, the nanoparticles can enter the water environment and adsorb substantial amounts of contaminants owing to their large specific surface area. Cotton, wool, acrylic and nylon fabrics can be directly dyed by using surface modified carbon black (CB), self-dispersible carbon black (SDCB), nanoparticles through an exhaustion process. The SDCB nanoparticles were prepared by refluxing CB particles in nitric acid for certain time to result in hydrophilic carboxylic groups on their surfaces. The SDCB nanoparticles behaved similarly to direct or acid dyes in dyeing cotton, acrylic and nylon fibers[32].

Carbon black (CB) is a practically pure element of carbon, also called “soot” or “shouen.” CBs are the forms of colloidal particles, manufactured by partial combustion or thermal decomposition of oil or gas, with an excessive deal of oxygen inside large furnaces under controlled environments. By changing the amount of oil and air, the temperature will be affected and as a result different particle size and connection of CBs will be produced.

Carbon blacks physical appearance is finely divided into pellets or powders. CB materials are hydrophobic. They are often used to effectively trap organic compounds from water or under high humidity conditions; conditions where the performance of other sorbents is reduced. While activated carbon relies on its high surface-area-to-volume ratio to adsorb organic compounds, the surface interactions of CB depend solely on dispersion forces. CB materials have been used to trap a wide range of organic compounds from C4 hydrocarbons to polychlorinated biphenyls (PCBs) [15]. Typically, compounds are adsorbed on the CB surface from large volumes of air

or water, and then subsequently released either by solvent desorption or thermal desorption resulting in either a concentration of the analytes, solvent exchange or combination of both.

Due to the polymorphism of carbonaceous materials and the versatility of the C-F bonding, the carbon/fluorine combination in fluorinated carbons is a quite unique association in chemistry. This results in interesting materials for many technological applications such as electrode materials for lithium batteries and solid lubricants. When these fluorinated carbons are used as electrode materials in primary lithium battery, the modulation of both the covalence of the C-F bonding and the fluorine content allows either high capacities, high discharge potentials or highpower densities to be obtained as a function of the application[32].

The CB powders mainly have two distinct properties, including physicochemical properties and compound properties:

Physicochemical Properties:

- Particle Size: The smaller the carbon black, the larger the specific surface is.
- Structure: The greater the oil absorption, the more multifaceted the arrangement is.
- Surface Chemistry: Different functional groups such as hydroxyl and carboxyl group can be found in the surface of the carbon black and this can change the compound characteristics.
- Aggregate Distribution: The size of the aggregates can vary, and if the distribution is spiky then there are many aggregates of the same size.

Compound Properties:

- Reinforcement: CB powder is added to many materials to increase strength, such as rubber used in tires or high pressure hoses as a material reinforcement.
- Conductivity: Adding CB to natural rubber results in a decrease of resistance in their electrical resistance. This conductivity is because of the channels of electrons jumping from one particle to another.

- Pigmentation: CB powder has physically powerful tint properties, because thermal stability makes it suitable for plastic and film coloring. This property of CB comes from its size and structural interaction with light.
- UV-light Protective Properties: UV-light can be absorbed by CB, and this protects the polymeric materials from degradation. This is because the CB stress-fissure prevention in plastics refines their crystals.

The study of the tribologic properties of fluorinated GCBs shows that fluorination improves the lubricating performances of the compounds. Highly fluorinated materials (F/C[0.6]) present the best intrinsic friction properties. The decrease of the intrinsic friction coefficient observed when the F/C ratio increases in the range 0–0.6 suggests that friction mechanisms involve surface effects in the early stage of friction [34].

CB and FCB can be used in Biomedical engineering application for theranostics application due to the surface ratio availability and less cytotoxic[35]. Cytotoxicity and biodegradability could be altered by functionalising the surface with Hydrophilic group and the core with hydrophobic to enhance drug or molecule suspension. Carbon black stable suspension is required to achieve varied application.

## 1.5 HYDROPHOBINS AS DISPERSIVE AGENTS FOR CARBON MATERIALS

Graphene has attracted vast interest as a new material with many uses. Two-dimensional, crystalline graphene has many advantageous properties, such as extremely high electric and thermal conductivity, high strength, and a large surface area. Many more useful properties can result graphene assemblies and modification by different functionalities or additional molecules. One of the usual ways to functionalize graphene is chemical modification, however, attempts to modify the surface of graphene in a noncovalent, nondestructive way have also been successful. These methods typically involve the buildup of charge on the graphene surface to enable the stabilization and assembly of the graphene sheets based on electrostatic interactions [14]. Class I fungal Hydrophobins are small surface-active proteins that self-assemble to form amphipathic

monolayers composed of amyloid-like rodlets. The monolayers are extremely robust and can adsorb onto both hydrophobic and hydrophilic surfaces to reverse their wettability. This adherence is particularly strong for hydrophobic materials. It has been reported that by Wenrong Yang et al. the class I Hydrophobins EAS and HYD3 can self-assemble to form a single-molecule thick coating on a range of nanomaterials, including single-walled carbon nanotubes (SWCNTs), graphene sheets, highly oriented pyrolytic graphite, and mica [7]. Moreover, coating by class I hydrophobin results in a stable, dispersed preparation of SWCNTs in aqueous solutions. No cytotoxicity is detected when hydrophobin or hydrophobin-coated SWCNTs are incubated with Caco-2 cells in vitro. In addition, the study shows that are able to specifically introduce covalently linked chemical moieties to the hydrophilic side of the rodlet monolayer. Hence, class I hydrophobins provide a simple and effective strategy for controlling the surfaces of a range of materials at a molecular level and exhibit strong potential for biomedical applications.

One of the main challenges in the production of graphene is the scalable, controllable, and safe processing and handling of individual graphene sheets. Methods for the fabrication of graphene in a dry environment include the micromechanical cleavage of graphene sheets from graphite and the epitaxial growth of graphene on certain substrates. By these methods, very large entities of single-layer graphene can be produced, but the scalability and handling problems remain. High-yielding solution-based chemical methods that enable the handling of graphene in dispersed form. In the presence of surfactants, it offers a promising production of graphene. The main benefits of solution methods are the better processability and increased safety of graphene when it is dispersed in a liquid instead of being used as a dry powder. The dispersion of graphene into aqueous solutions is especially attractive because of their nonvolatile nature. Functionalization is achieved by adding Hydrophobin. HFBI which belongs to a class of proteins, interacts strongly with hydrophobic surfaces, such as graphite and silicon. The protein has a strongly cross-linked fold containing four disulfide bridges. Its most striking feature is a patch of hydrophobic residues on one face of its structure. Thus, the protein resembles a typical surfactant with a hydrophilic and a hydrophobic part. In solution, hydrophobic interactions between individual proteins lead to the formation of dimers or tetramers. In the vicinity of the



interface between water and air. The sonication of mixtures of HFBI and graphite produces thin graphene-like hybrid structures. The use of genetically engineered HFBI should enable specific modification of the graphene surface with both biological and non-biological functionalities, including molecules capable of specific recognition or actuated responses. The possibility of using a layer of adsorbed molecules to affect the electrical properties of graphene makes this hybrid material especially attractive for electronic and sensor applications [14].

According, to the study conducted by Katri Kurppa et al., HFBI showed efficient solubilization and functionalization of SWNTs, an engineered variant NCysHFBI increases the functionalization and dispersion. This interaction allowed the formation of novel protein–SWNT composite films as well as hybrid nanostructures of carbon nanotubes and AuNPs. This opens a route for combining their optical and electronic functions in new ways and can form a valuable addition to the toolbox of biomolecules that are finding use in nanotechnology [17].

## 1.6 OBJECTIVE OF THIS PROJECT

The main objective of this thesis is to exploit the use of Hydrophobin as a surfactant to prepare stable aqueous dispersions of carbon nanomaterials which are not soluble in water. This project focuses on using class 2 Hydrophobin HFBI and graphitized carbon blacks (CB), both fluorinated (F-CB) and non fluorinated (CB), making them water-dispersible as detailed in the following sections of the thesis. CBs should be dispersed homogeneously, so that they can be used in different applications. For this purpose, Hydrophobins have been used as a surfactant. Its solution in MilliQ water was mixed with carbon blacks. To enhance the dispersion stability of the carbon nanomaterials, two different experimental protocols were tested. The resulting dispersions were analyzed with DLS, TEM and FTIR. The results have been optimized by increasing or decreasing the concentration of HFBI and by tuning the process parameters. If CBs are stable in water without aggregating, then this preliminary study would open doors for many new applications.

## 2. MATERIALS AND METHODS

### 2.1 MATERIALS

Hydrophobin II (HFB II) was provided by VTT Technical Research Centre of Finland and it was stored under vacuum in a falcon tube sealed with Parafilm®.

Non-fluorinated and fluorinated carbon blacks were kindly provided by Prof. Marc Dubois (Laboratoire Commun de Recherche UCA/CNRS/AREVA, Clermont-Ferrand, France).

Ethanol and chloroform of commercial purity grade were used as received. Ultrapure Type I Milli-Q water (mQw, 18.2 M $\Omega$ /cm) was obtained from a Simplicity (Millipore) filtration apparatus.

### 2.2 METHODS

Particle size distribution of carbon blacks was characterized by Multiangle Dynamic Light Scattering (DLS), using an ALV apparatus equipped with ALV-5000/EPP Correlator, special optical fiber detector and ALV/CGS-3 Compact goniometer. The light source is He-Ne laser ( $\lambda$  = 633 nm), 22 mW output power. Measurements were performed at 25 °C. Approximately 1 mL of sample was transferred into a cylindrical Hellma scattering cell. Data analysis has been performed according to standard procedures and auto-correlation functions were analysed through a constrained regularization method (Laplace inversion of the time auto-correlation functions), CONTIN, for obtaining the particle size distribution.

Transmission Electron Microscopy (TEM) images were acquired with a DeLong America LVEM5 microscope, equipped with a field emission gun and operating at 5 kV.

Attenuated Total Reflectance Fourier-Transform Infrared spectroscopy (ATR-FTIR) spectra were obtained with a Thermo Scientific Nicolet iS50 FTIR spectrometer, equipped with an iS50 ATR accessory (Thermo Scientific, Madison, USA). The values were given in wavenumbers and were rounded to 1 cm<sup>-1</sup> upon automatic assignment.

$^{19}\text{F}$ -NMR spectra were recorded at 305 K on a Bruker AV400 spectrometer operating at 400 MHz for the  $^{19}\text{F}$  nucleus, in order to assess the effective presence of fluorinated carbon blacks dispersed in water.

### 2.2.1 Dynamic Light Scattering

Dynamic Light Scattering (DLS, also known as Photon Correlation Spectroscopy or Quasi-Elastic Light Scattering) is one of the most popular light scattering techniques because it allows particle sizing down to 1 nm diameter. It is an optical technique used for analyzing dynamic properties and size distribution of a broad variety of physical, chemical and biological systems composed of several suspended constituents [21]. These can be colloidal particles, macromolecules, bubbles or droplets.

DLS is based on the extraction of spectral information derived from time-dependent fluctuations of the light scattered from a spatially limited volume within the sample. Specifically, when a suspension of particles is hit by a monochromatic coherent beam of light, generated scattered light waves spread out in all directions. Scattered waves interference in the far field region generates a net scattered light intensity  $I_s(t)$ . Due to the random motion of the suspended particles within the sample, the interference can be stochastically either constructive or destructive, hence resulting in a stochastic light intensity signal.

The suspended particles of the colloidal dispersion under investigation undergo Brownian motion. This motion results in fluctuations in the distances between the particles and hence also in fluctuations of the phase relations of the scattered light. Additionally, the number of particles within the scattering volume may vary in time. The net result is a fluctuating scattered intensity.

Simple DLS instruments that measure at a fixed angle can determine the mean particle size in a limited size range. More elaborated multi-angle instruments can determine the full particle size distribution.

From a microscopic point of view, the particles scatter the light and thereby imprint information about their motion. Analysis of the fluctuation of the scattered light thus yields information about the particles. Experimentally one characterizes intensity fluctuations by computing

the intensity correlation function  $g_2(t)$ , whose analysis provides the diffusion coefficient of the particles (also known as diffusion constant).

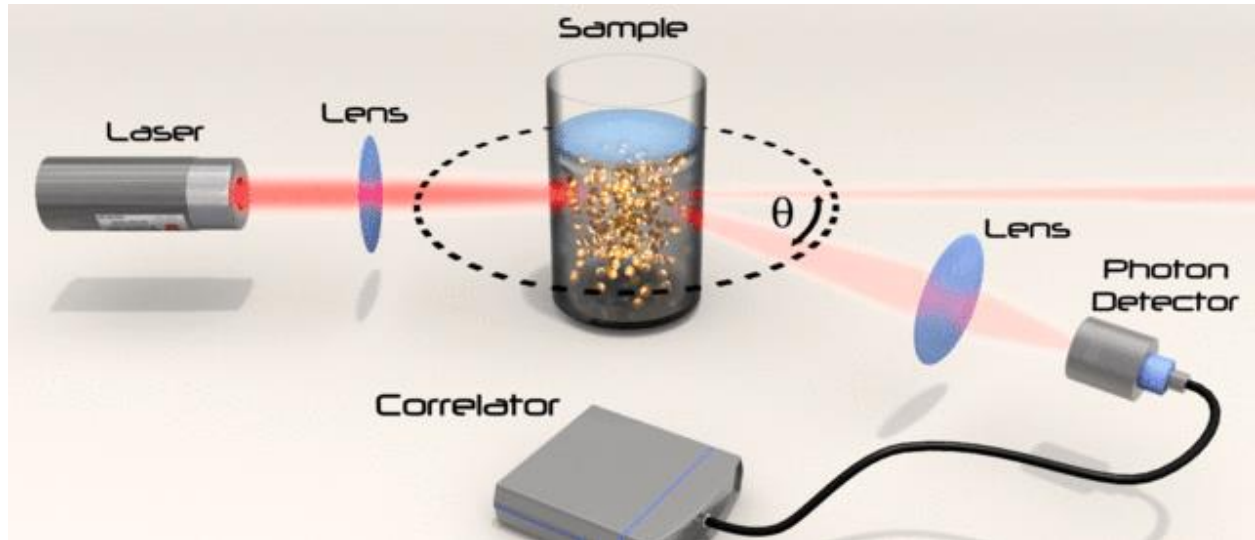


Figure 5. Dynamic Light Scattering instrument setup (Copyright LSI)

The diffusion coefficient  $D$  is then related to the radius  $R$  of the particles by means of the Stokes-Einstein Equation:  $D = \frac{K_B T}{6\pi\eta R_H}$

$$6\pi\eta R_H$$

Where  $K_B$  is the Boltzmann constant,  $T$  the temperature and  $\eta$  the viscosity.

The correlation of the intensity can be performed by electronic hardware (digital correlator) or software analysis of the photon statistics. Because fluctuation is typically in the range of nanoseconds to milliseconds, electronic hardware is typically faster and more reliable at this job.

The quality of a DLS measurement depends on several factors. Some obvious, such as the quality of the components (the laser, the detector, the correlator...), other factors are not as straightforward but may influence the measurement significantly. Some important points to be considered are listed below.

The decay rate depends on the wave vector and thus the scattering angle. Particles of different sizes scatter with different intensities in dependence of the scattering angle. Thus there is an optimum angle of detection for each particle size. A high-quality analysis should always be performed at several scattering angles (multiangle DLS). This becomes even more important in case of polydisperse samples with unknown particle size distribution since, at certain angles, the scattering intensity of some particles will completely overwhelm the weak scattering signal of other particles, thus making them invisible to the data analysis at this angle.

In this work, analysis were performed at four different angles i.e 70°, 90°, 110°, 130°. Sample volumes of 1 mL were used. Concentration of the sample plays a important role in the measurement of particle size and distribution, and so in some cases samples were diluted before analysis.

### 2.2.2 ATR-FTIR

IR spectroscopy is the oldest and most commonly used method for identifying both organic and inorganic chemicals, as well as for providing specific information on molecular structure, chemical bonding, and molecular environment. Being a powerful tool for qualitative and quantitative studies, it can be applied to study solids, liquids, or gaseous samples [22]. Recently, IR spectroscopy has been applied *in situ* to study surface reactions on immersed solids such as oxides. This has been achieved with particle films via internal reflection or attenuated total reflection (ATR-FTIR) methods. Investigating several metal oxide solid particles in suspensions or deposited as thin films on ATR crystals, these developments have led to *in situ* ATR-FTIR studies of adsorption and chemical reactions on a variety of solid-liquid and/or solid-gas interfaces [23].

Attenuated total reflection (ATR) is a sampling technique used in conjunction with infrared spectroscopy which enables samples to be examined directly in the solid or liquid state without further preparation. A beam of infrared light is passed through the ATR crystal in such a way that it reflects at least once off the internal surface in contact with the sample. This reflection forms the evanescent wave which extends into the sample. The penetration depth into the sample is typically between 0.5 and 2 micrometres, with the exact value being determined by the

wavelength of light, the angle of incidence and the indices of refraction for the ATR crystal and the medium being probed [27]. The number of reflections may be varied by varying the angle of incidence. The beam is then collected by a detector as it exits the crystal. Most modern infrared spectrometers can be converted to characterise samples via ATR by mounting the ATR accessory in the spectrometer's sample compartment. ATR spectroscopy was introduced simultaneously by Harrik [24] and Fahrenfort [25] based upon the total internal reflection phenomena. In this approach, IR spectra are recorded for a sample material that is in contact with an internal reflection element (IRE). The IR beam is focused onto the edge of the IRE, reflected through the IRE, and then directed to the detector. In this case, all the light reflects off the internal surface of the IRE, hence explaining the term total internal reflection. The internal reflection element (IRE) or ATR crystal has, in most cases, a higher refractive index ( $n_1$ ) as compared to the sample ( $n_2$ ). Another important parameter is the incidence angle  $\theta$  that can be determined from the refractive indexes of the sample ( $n_2$ ) and the IRE ( $n_1$ ).

The major applications of the ATR method are in the mid-IR region. However, the range has been extended to the near-IR, the far-IR, as well as to the UV and visible spectral regions. Therefore, it is of great importance to choose a suitable ATR crystal for a given application.

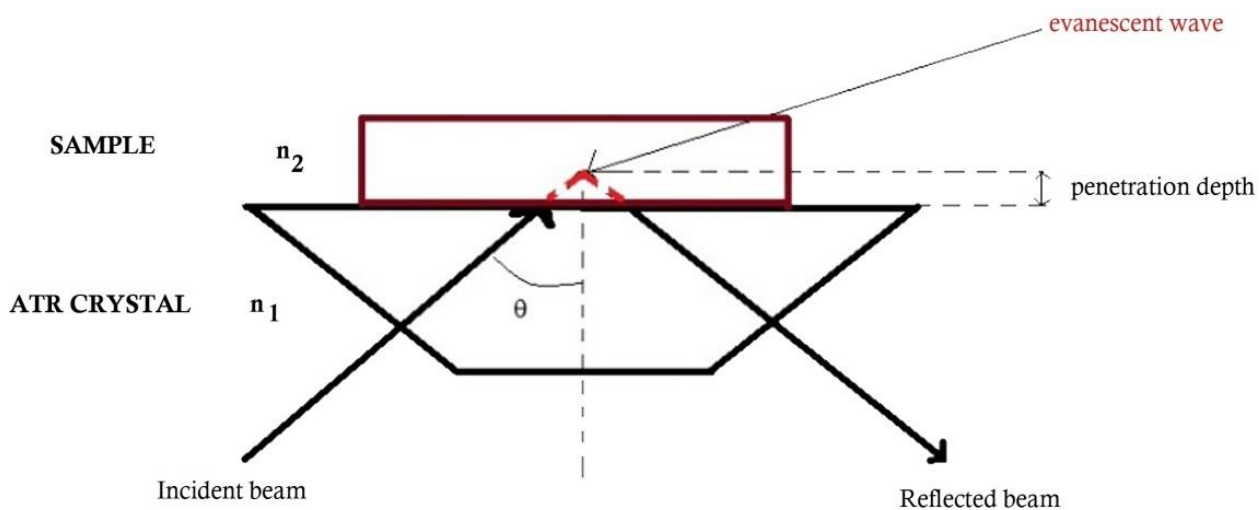


Figure 6. Schematic diagram of a horizontal ATR sampling accessory illustrating the important parameters [26]

Infrared (IR) spectroscopy by ATR is applicable to the same chemical or biological systems as the transmission method. One advantage of ATR-IR over transmission-IR is the limited path length into the sample. This avoids the problem of strong attenuation of the IR signal in highly absorbing media such as aqueous solutions. For ultraviolet or visible light (UV/Vis) the evanescent light path is sufficiently short such that interaction with the sample is decreased with wavelength. For optically dense samples, this may allow for measurements with UV. Also, as no light path has to be established single shaft probes are used for process monitoring and are applicable in both the near and mid infrared spectrum.

Infrared (IR) spectroscopy by ATR is applicable to the same chemical or biological systems as the transmission method. One advantage of ATR-IR over transmission-IR is the limited path length into the sample. This avoids the problem of strong attenuation of the IR signal in highly absorbing media such as aqueous solutions. For ultraviolet or visible light (UV/Vis) the evanescent light path is sufficiently short such that interaction with the sample is decreased with wavelength. For optically dense samples, this may allow for measurements with UV. Also, as no light path has to be established single shaft probes are used for process monitoring and are applicable in both the near and mid infrared spectrum.



*Figure 7. Thermo Fisher Nicolet iS50 FTIR Spectrometer (Example of the complete instrument; copyright imrt)*

Typical materials for ATR crystals include germanium, KRS-5 and zinc selenide, while silicon is ideal for use in the Far-IR region of the electromagnetic spectrum. The excellent mechanical properties of diamond make it an ideal material for ATR, particularly when studying very hard solids, but its much higher cost means it is less widely used. The shape of the crystal depends on the type of spectrometer and nature of the sample. With dispersive spectrometers, the crystal is a rectangular slab with chamfered edges, seen in cross-section in the illustrations. Other geometries use prisms, half-spheres, or thin sheets.

In this study, samples were analysed to check whether HFBII forms film around the CB and F-CB. At the beginning HFBII and crude samples of both F-CB and CB were analysed separately. Then F-CB and CB in HFBII mixture were analysed to confirm the presence of HFBII onto the nanoparticles.

### 2.2.3 TEM (Transmission Electron Microscopy)

Nanoscale structures are very difficult to view through a conventional light microscope. Transmission Electron Microscopy (TEM) is a powerful technique to examine some fine features whose characteristic dimensions are less than 100 nm in size [28]. TEM has been widely applied in the fields of biological and material science and engineering. Ernst Ruska developed the first electron microscope, a TEM, with the assistance of Max Knolls in 1931. After significant improvements to the quality of magnification, Ruska joined the Siemens Company in the late 1930s as an electrical engineer, where he assisted in the manufacturing of his TEM.

TEMs consist of the following components:

- An electron source
- Thermionic Gun
- Electron beam
- Electromagnetic lenses
- Vacuum chamber
- 2 Condensers



- Sample stage
- Phosphor or fluorescent screen
- Computer

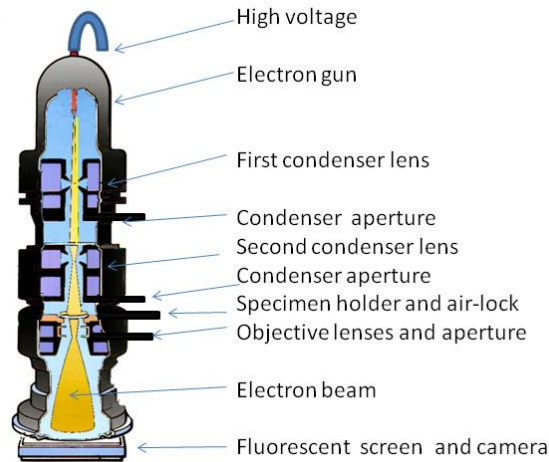


*Figure 8. Simplified diagram of a transmission electron microscope. Drawing by Graham Colm, courtesy of Wikimedia Commons.*

A Transmission Electron Microscope produces a high-resolution, black and white image from the interaction that takes place between prepared samples and energetic electrons in the vacuum chamber. The beam of electrons from the electron gun is focused into a small, thin, coherent beam by the use of the condenser lens. This beam is restricted by the condenser aperture, which excludes high angle electrons. The beam then strikes the specimen and parts of it are transmitted depending upon the thickness and electron transparency of the specimen. This transmitted portion is focused by the objective lens into an image on phosphor screen or charge coupled device (CCD) camera. Optional objective apertures can be used to enhance the contrast by blocking out high-angle diffracted electrons [28]. The image then passed down the column through the intermediate and projector lenses, is enlarged all the way.

The image strikes the phosphor screen and light is generated, allowing the user to see the image. The darker areas of the image represent those areas of the sample that fewer electrons are transmitted through while the lighter areas of the image represent those areas of the sample that more electrons were transmitted through.

Air needs to be pumped out of the vacuum chamber, creating a space where electrons are able to move. The electrons then pass through multiple electromagnetic lenses. These solenoids are tubes with coil wrapped around them. The beam passes through the solenoids, down the column, makes contact with the screen where the electrons are converted to light and form an image. The image can be manipulated by adjusting the voltage of the gun to accelerate or decrease the speed of electrons as well as changing the electromagnetic wavelength via the solenoids.

The coils focus images onto a screen or photographic plate. During transmission, the speed of electrons directly correlates to electron wavelength; the faster electrons move, the shorter wavelength and the greater the quality and detail of the image. The lighter areas of the image represent the places where a greater number of electrons were able to pass through the sample and the darker areas reflect the dense areas of the object. These differences provide information on the structure, texture, shape and size of the sample. To obtain a TEM analysis, samples need to have certain properties. They need to be sliced thin enough for electrons to pass through, a property known as electron transparency.

Samples need to be able to withstand the vacuum chamber and often require special preparation before viewing. Types of preparation include dehydration, sputter coating of non-conductive materials, cryofixation, sectioning and staining.

In this study, a low-resolution Transmission Electron Microscope (TEM) was used to acquire images of the starting F-CB and CB, and then images of the same carbon blacks dispersed in aqueous HFBII, to check whether the protein formed a film around the carbon particles. TEM samples were prepared by dropping 50-100  $\mu$ L of sample on a copper grid (200 or 400 mesh) placed on filter paper. The grid was left to dry overnight for evaporating the solvent, and then inserted in the microscope chamber.

## 2.2.4 NMR (Nuclear Magnetic Resonance)

Nuclear Magnetic Resonance (NMR) spectroscopy is an analytical chemistry technique used in quality control and research for determining the content and purity of a sample as well as its molecular structure. For example, NMR can quantitatively analyze mixtures containing known compounds. For unknown compounds, NMR can either be used to match against spectral libraries or to infer the basic structure directly. Once the basic structure is known, NMR can be used to determine molecular conformation in solution as well as studying physical properties at the molecular level [30].

The basic phenomenon of NMR spectroscopy is similar to other forms of spectroscopy, such as visible spectroscopy. A photon of light causes a transition from the ground state to the excited state. For example, in the case of visible spectroscopy the absorption of a photon by an electron causes the electron to move from its ground state orbital to an orbital of higher energy, the excited state. In the case of NMR, the absorption of a radio-frequency photon promotes a nuclear spin from its ground state to its excited state. NMR spectroscopy differs in a number of important aspects from other forms of spectroscopy.

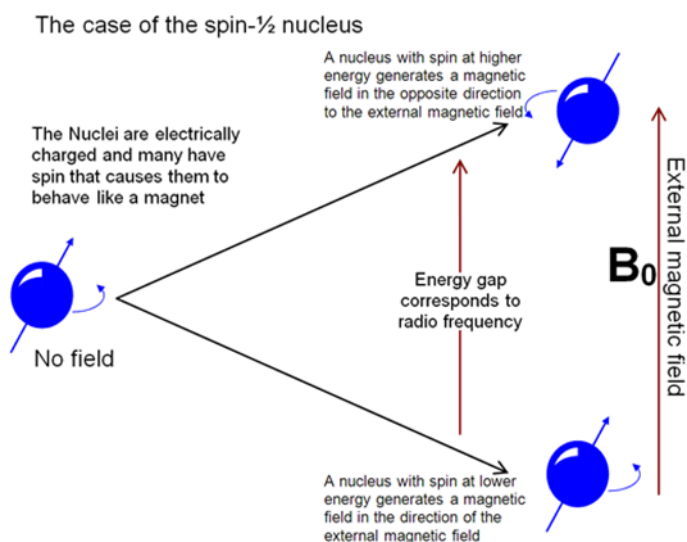


Figure 9 NMR spin- $\frac{1}{2}$  nuclei model

Figure 9. Behavior of spin- $1/2$  nuclei in the presence of an external magnetic field, including the most commonly used NMR nucleus (proton,  $^1\text{H}$ ), as well as many other nuclei such as  $^{19}\text{F}$ ,  $^{13}\text{C}$ ,  $^{15}\text{N}$  and  $^{31}\text{P}$  [30].

First, the generation of the ground and excited NMR states requires the existence of an external magnetic field. This requirement is a very important distinction of NMR spectroscopy in that it allows one to change the characteristic frequencies of the transitions by simply changing the applied magnetic field strength. Second, the NMR excited state has a lifetime that is on the order of  $10^9$  times longer than the lifetime of the excited electronic states.

The NMR experiment measures a large ensemble of spins derived from a huge number of molecules. Therefore, we now look at the macroscopic behaviour. The sum of the dipole moments of all nuclei is called magnetization. In equilibrium the spins of  $I=1/2$  nuclei are either in the  $\alpha$ - or  $\beta$ -state and precess about the axis of the static magnetic field. However, their phases are not correlated. For each vector pointing in one direction of the transverse plane a corresponding vector can be found which points into the opposite direction.

A particularly useful class of reporter groups contain fluorine atoms that can be investigated by rather straightforward  $^{19}\text{F}$  NMR experiments. In contrast to other popular NMR active nuclei, such as  $^1\text{H}$ ,  $^{13}\text{C}$ ,  $^{15}\text{N}$  or  $^{31}\text{P}$ , fluorine is not a natural component of biological macromolecules and can thus be used as a site-specific reporter of high sensitivity that reports on the structure, dynamics and ligand-interaction of complex biological systems. In this work,  $^{19}\text{F}$  NMR was used to identify the presence of fluorine atoms in the aqueous dispersions of fluorinated carbon blacks, to confirm the effective dispersing activity of HFBII [31].

# 3. RESULTS AND DISCUSSION

## 3.1 DISPERSION OF CARBON BLACKS (CB) AND FLUORINATED CARBON BLACKS (FCB) IN ORGANIC SOLVENTS

Nanomaterials such as carbon blacks (CB) and fluorinated carbon blacks (FCB) are generally dispersible in organic solvents such as ethanol or chloroform. The main aim is to disperse them in water without any chemical modification of their surface, usually the only way to obtain water-soluble carbon nanomaterials is to functionalize their surface with carboxylate groups.

As a control, starting carbon blacks (CB) and fluorinated carbon blacks (FCB) were suspended in ethanol by ultrasound (US) bath sonication (15 min) at a concentration of 0.06 mg/mL or in chloroform by magnetic stirring for 30 mins.



*Figure 10. Dispersion of carbon blackss in ethanol*



*Figure 11. Dispersion of fluorinated carbon blackss in ethanol*

Figure 10 shows the image of the vial with the starting CB suspended in ethanol. This carbon blacks dispersion was stable only for a small period of time, i.e. 15-30 minutes. After that, CBs started to precipitate at the bottom of the vial. Figure 11 shows the fluorinated carbon blacks (FCBs) dispersed in ethanol immediately after US treatment. Once again, after a short span of time FCBs started to settle down in the vial. After the simple analysis by visually checking the vial, samples were then characterized using DLS, ATR-FTIR, and TEM to make the comparison easier between the dispersion in solvent and dispersion in MilliQ water with HFBII.

### 3.1.1 TEM IMAGES OF THE STARTING CARBON BLACKS AND FLUORINATED CARBON BLACKS IN ORGANIC SOLVENTS

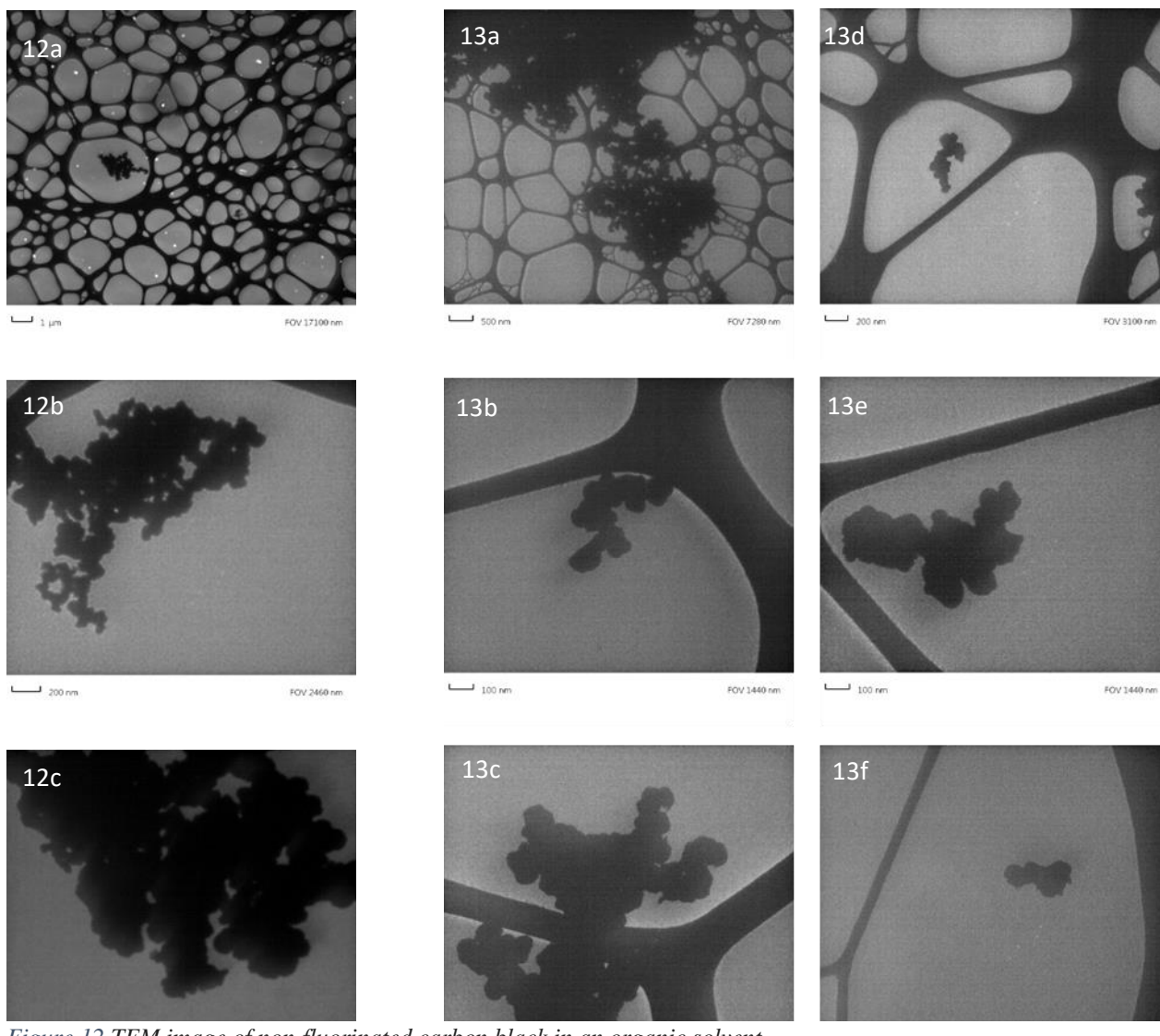


*Figure 12 TEM image of non-fluorinated carbon black in an organic solvent*

*Figure 13 TEM image of fluorinated Carbon blacks in an organic solvent*

TEM images show the morphology and particle distribution of particles in the organic solvents. Figure 12(a-c) shows some TEM images of non-fluorinated CBs in ethanol. Black spheres are the nanoparticles of carbon blacks. There is a significantly large amount of aggregation between the particles. Mean diameter of a single carbon blacks particle is around 100-140 nm. Organic solvents such as ethanol and chloroform do not have any effect on the particles. Figure 13(a-f)

reports TEM images of fluorinated CBs in ethanol. Mean diameter of a single FCB particle is around 100-120 nm.

### 3.2. DISPERSION OF STARTING CBS IN AQUEOUS HYDROPHOBIN (HFBII) SOLUTION

Two samples of CB-HFBII solution were prepared with the same concentration. The first sample was kept in US bath sonicator for 30 minutes. The second sample was tip sonicated for 5 minutes using a SONIC Vibra-Cell tip sonicator (Newtown, CT) operating at 130 W and 20 kHz (70% amplitude), placing the sample's vial inside a beaker filled with ice to avoid overheating. The two samples of CBs prepared with the two different procedures were used to check the dispersion stability of CB with HFBII in MilliQ water.

CB dispersions (0.04 mg/mL) in a solution of HFBII (0.1 mg/mL) in MilliQ water were obtained by two different procedures:

- US bath sonication (30 min)
- Tip sonication (70% amplitude; 5 min; ice cooling)

Carbon nanomaterials remained suspended for at least 24 h before starting to precipitate.

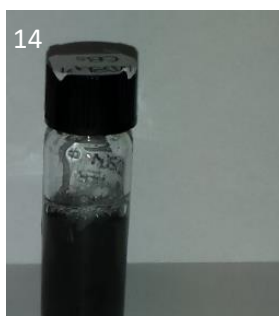


*Figure 14. Dispersion of carbon blacks in HFBII-MilliQ water*

The samples were then characterized using DLS, ATR-FTIR, TEM to make the comparison easier between the dispersion in organic solvent and dispersion in HFBII with MilliQ.

### 3.2.1 TEM IMAGES OF THE STARTING CARBON BLACKS IN HFBII-MilliQ WATER

TEM grids were prepared by dropping 50 mL of the sample, and were then let to dry under the hood for 24 hours. After 24 hours the grids were inserted into the TEM instrument. Two TEM grids were prepared, one with the sample prepared using US bath (30 minutes) and other with the sample prepared using tip sonicator (5 mins). Both samples were diluted 1:4 before dropping them on the TEM grids.

#### ULTRASOUND BATH TREATMENT    TIP SONICATION TREATMENT

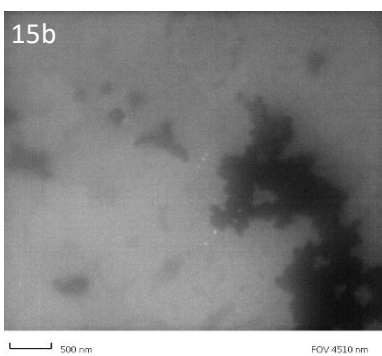
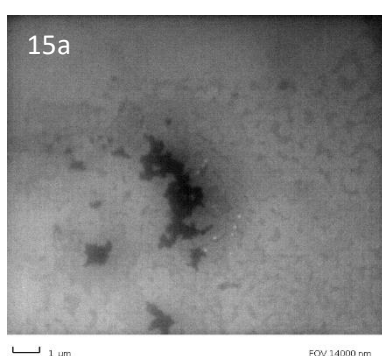


*Figure 15(a-b). TEM images of CBs in HFBII-MilliQ prepared using US bath for 30 minutes.*

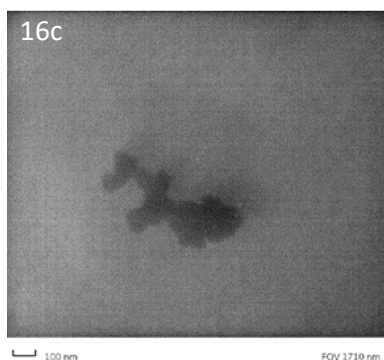
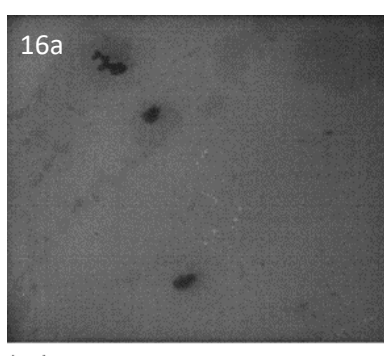


*Figure 16(a-c). TEM images of CBs in HFBII-MilliQ prepared using tip sonication for 5 minutes.*



TEM images show a comparison between carbon blacks/HFBII-MilliQ solution treated with ultrasound bath for 30 minutes (Fig. 15) and carbon blacks/HFBII-MilliQ solution treated with tip sonication (Fig. 16). Both Figures show that HFBII actually formed a film around CBs, making them suspended in MilliQ not as isolated particles but as aggregates of particles. Figure 15(a-b) shows that the carbon blacks suspension in HFBII-MilliQ prepared using US bath seems to be characterized by bigger aggregates compared to the one prepared using tip sonication (Figure 16, a-c), probably due to the fact that energy in this latter case was directly applied to the sample bulk. Both samples showed increased suspension stability (up to 24 hours) if compared to CBs dispersed in ethanol, which could be a good starting point for protocol optimization. Dispersions obtained through tip sonication were slightly more stable in time than those prepared using ultrasound bath.

### 3.2.2 ATR-FTIR ANALYSIS OF THE STARTING CARBON BLACKS IN HFBII-MilliQ WATER

Attenuated Total Reflectance FT-IR spectra were collected for the following samples: CB powder, HFBII dissolved in MilliQ water (0.1 mg/mL), and CB with HFBII in water, as shown in Figure 17. For samples in solution, a drop was deposited on the ATR probe and the solvent

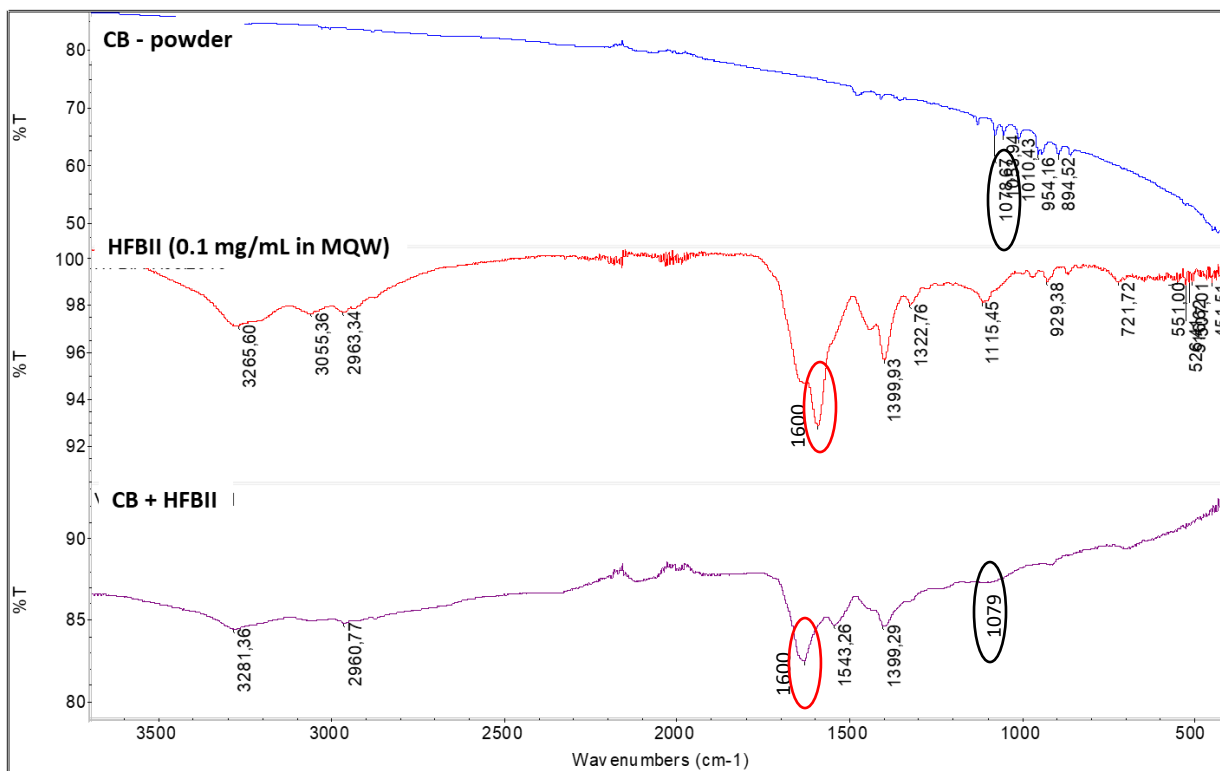


Figure 17. ATR-FTIR spectra of Crude carbon blacks powder, HFBII in MilliQ and the sample (CB+HFBII) was evaporated; several dropping and evaporation cycles were repeated in order to obtain a film of the sample on the probe. The dispersion of CBs with HFBII in MilliQ exactly matched the spectra of both HFBII and CB powder, as expected. CB is composed of 90-99% elemental carbon, with oxygen and hydrogen as the other major constituents, which can be distributed in the carbonaceous matrix in various organic functional groups such as hydroxyl (-OH), carbonyl (C=O) and carboxyl (COOH). In addition to these elements, CB may contain small amounts of nitrogen and sulfur, depending upon the nature of hydrocarbons used in the manufacture. The characteristic peaks are the C=O stretches in the range of 1300-1000 cm<sup>-1</sup>. The main peaks visible in the spectrum of the HFBII in solution are the Amide I band (1600 cm<sup>-1</sup>), mainly

associated with the C=O stretching vibration. FT-IR analysis (Figure 17) confirmed the simultaneous presence of both HFBII and CBs in the final water dispersion.

### 3.2.3 DLS ANALYSIS OF THE STARTING CARBON BLACKS IN HFBII-MilliQ WATER

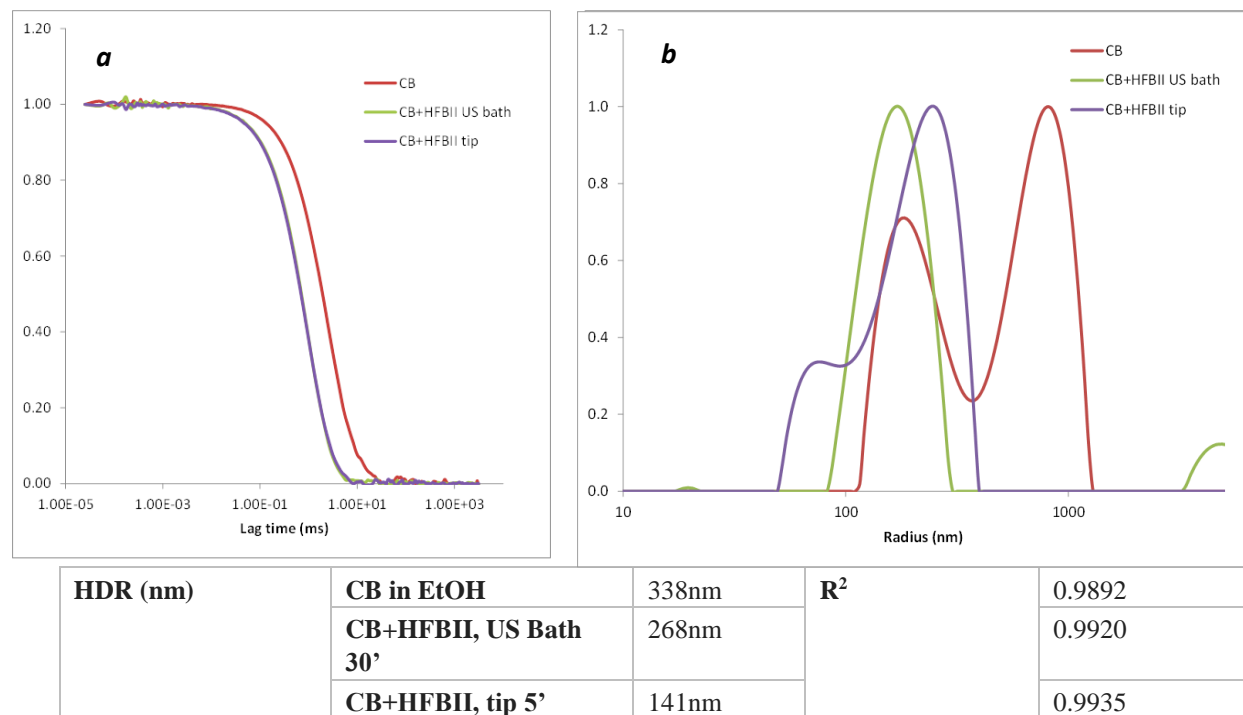


Figure 18. DLS comparison between carbon blacks suspended in ethanol and in HFBII-MilliQ: a) Correlation function at 90° b) Intensity-weighted average size distribution at 90° obtained by CONTIN fit.

Dynamic Light Scattering analysis (DLS) graphs the size distribution of particles in solution. Figure 18a shows that the correlation functions at 90° of CBs dispersed in organic solvent (red line), CBs in HFBII-MilliQ dispersed by 30 min US bath (green line), and CBs in HFBII-MilliQ prepared by 5 min tip sonication (purple line). Figure 18b compares the intensity-weighted average hydrodynamic radius at 90° calculated by CONTIN fit for the same three samples. DLS data show that CB particles coated by HFBII in water have a smaller average size and are more monodisperse, if compared to their suspension in organic solvent, independently from the dispersion protocol used (US bath or tip sonication). This observation is in agreement with TEM analyses and with the different stability observed for the samples. Whereas CBs in organic

solvents showed a strong tendency to sediment quite immediately, their dispersions in an aqueous solution of HFBII were quite stable for almost 24 hours.

### 3.3. DISPERSION OF FLUORINATED CARBON BLACKS (FCB) IN HYDROPHOBIN (HFBII) SOLUTION

Two samples of FCB-HFBII dispersions with the same concentration were prepared following the same two sonication procedures previously described for CBs.

FCB dispersions (0.06 mg/mL) in a solution of HFBII (0.1 mg/mL) in MilliQ water were obtained by two different procedures:

- US bath sonication (30 min)
- Tip sonication (70% amplitude; 5 min; ice cooling)

FCBs remained suspended for at least 24 h before starting to precipitate. Figure 19 shows the solution of HFBII in MilliQ containing fluorinated carbon blacks, which looked clear and showed no precipitation.



*Figure 19. Dispersion of fluorinated carbon blacks in HFBII-MilliQ water.*

Fluorinated carbon blacks remained suspended in HFBII-MilliQ water for almost 24 hours, proving that HFBII increased their dispersibility in aqueous environment.

#### 3.3.1 TEM IMAGES OF FLUORINATED CARBON BLACKS IN HFBII-MilliQ WATER

TEM images were taken to know the morphology and distribution of FCBs after suspension in water with HFBII. Both samples were analysed to check the efficiency of the dispersion

protocol. Samples were dropped onto TEM grids without dilution. TEM images show a comparison between the FCB/HFBII-MilliQ dispersion prepared by ultrasound bath and that obtained by tip sonication. Figure 20(a-d) shows that FCBs in HFBII-MilliQ solution prepared using ultrasound bath for 30 minutes are better dispersed than their non-fluorinated analogues under the same conditions.

### ULTRASOUND BATH FOR 30 min

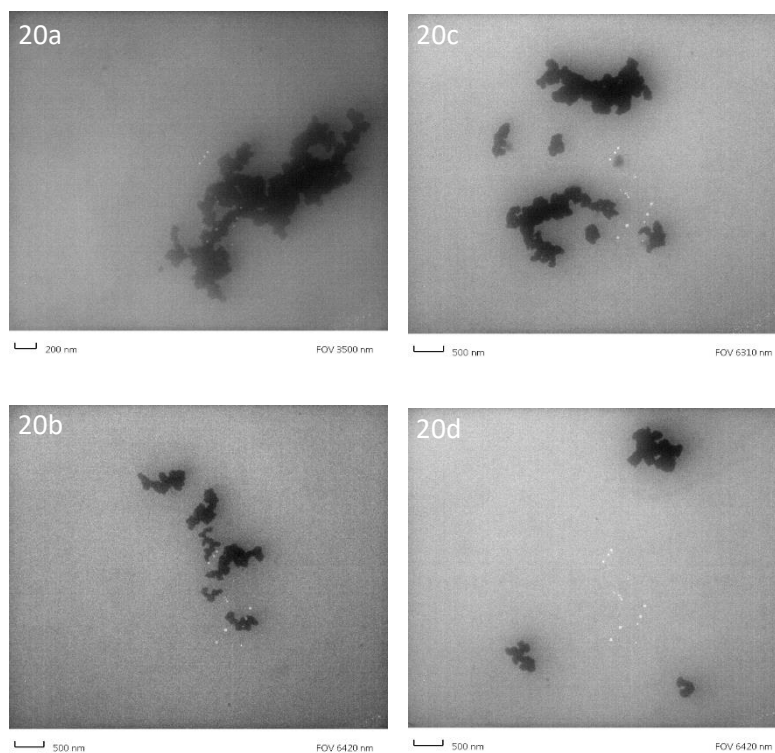


*Figure 20(a-d). TEM images of fluorinated carbon blacks (FCB) with HFBII in MilliQ water obtained after 30 min of ultrasound bath sonication.*

The size of the HFBII-coated aggregates of FCBs are smaller compared to those formed by CBs with HFBII. Size of these aggregates were roughly 500-750 nm. Lighter shade over the black colored region highlights that HFBII had formed a film around FCB aggregates, making their surface more hydrophilic.

## TIP SONICATION FOR 5 min

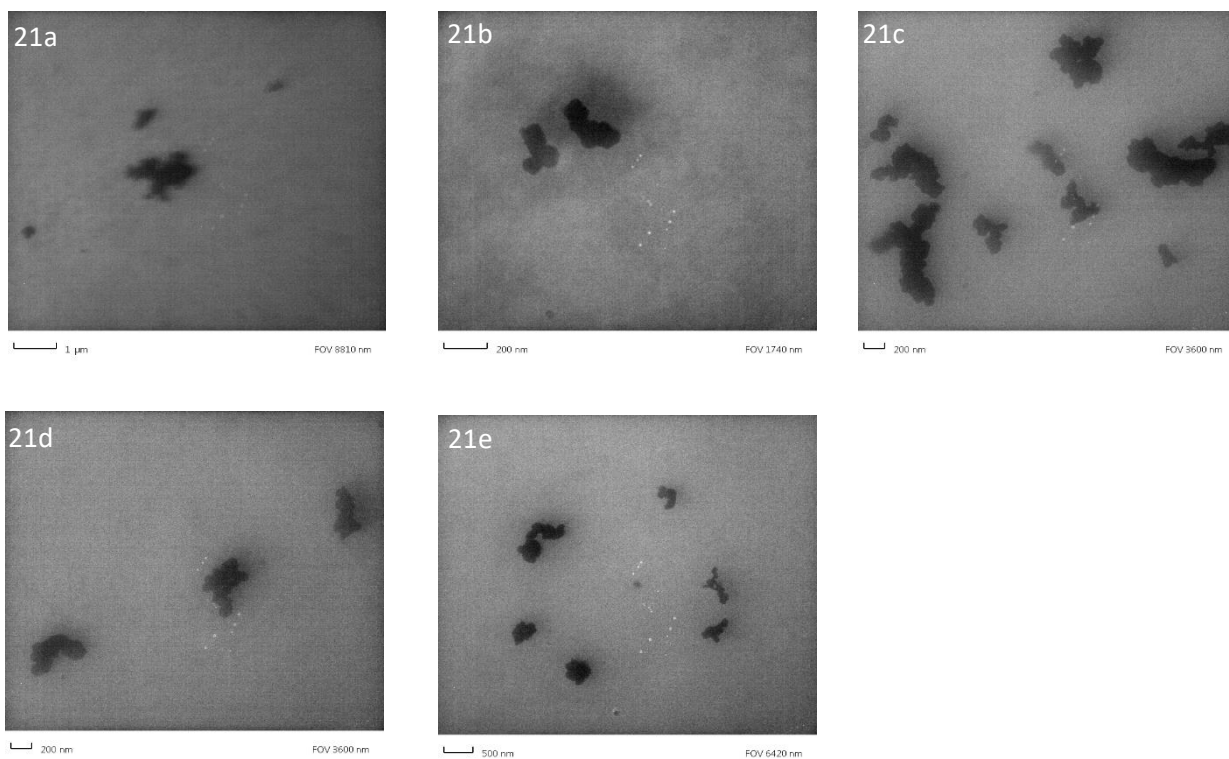


Figure 21(a-e). TEM images of FCBs with HFBII in MilliQ water obtained after tip sonication for 5 mins.

Figure 21(a-e) shows the TEM images of FCBs with HFBII in MilliQ treated with tip sonication for 5 minutes. Tip sonication treatment for suspending FCBs in HFBII with MilliQ actually enhanced their stability in dispersion. Black particles in the images are the FCBs, whereas the light color shadow surrounding them is due to the HFBII coating layer. From these images it emerges that the size of FCB aggregates were quite smaller compared to FCB-HFBII in MilliQ treated with ultrasound bath. Average size of the aggregated particles were around 250-350nm. These size were small and could be used for many applications. Even a few smaller aggregates of FCB particles were also present in the suspension.

### 3.3.2 ATR-FTIR ANALYSIS OF FLUORINATED CARBON BLACKS IN HFBII-MilliQ WATER

Attenuated Total Reflectance FT-IR spectra were collected for the following samples: FCB powder, HFBII dissolved in MilliQ water (0.1 mg/mL), and FCB with HFBII in MilliQ, as shown in Figure 22. The formulation of FCBs with HFBII in MilliQ exactly matched the spectra of both HFBII and FCB powder, as expected. FCBs are composed of carbon, hydrogen and fluorine. which can be distributed in the carbonaceous matrix in various organic

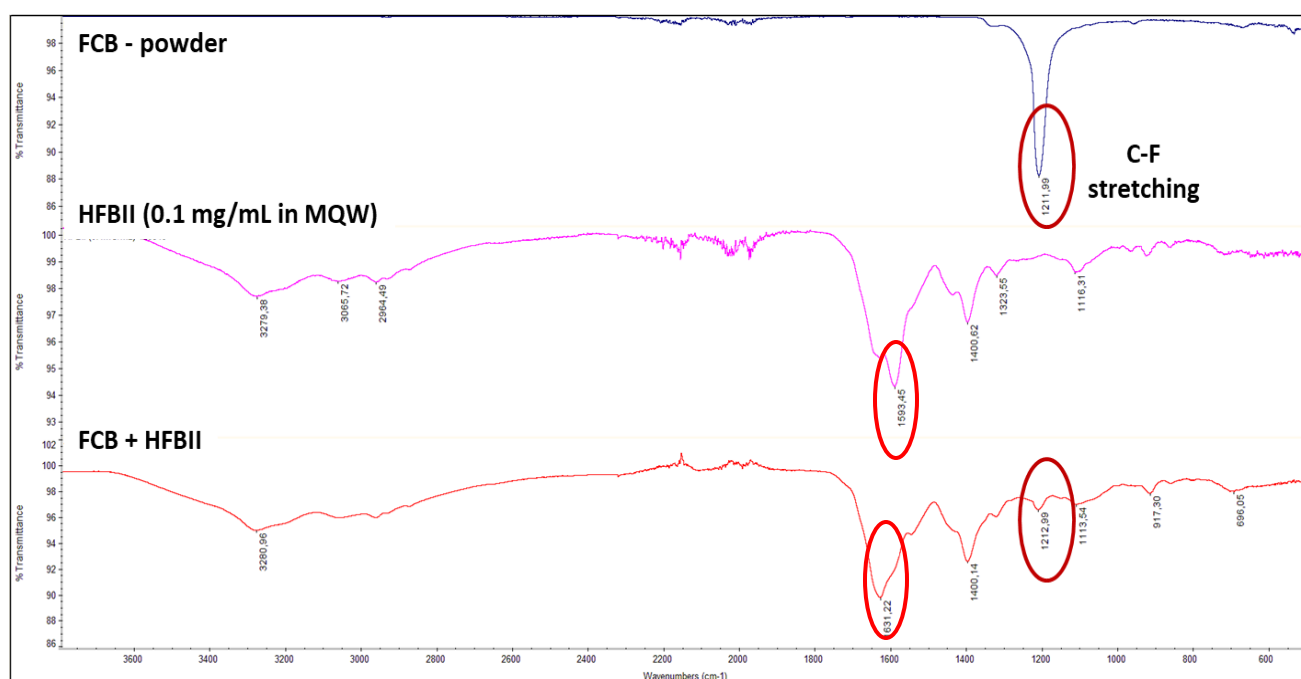


Figure 22 ATR-FTIR spectra of Fluorinated carbon blacks powder, HFBII in MilliQ and the sample (FCB+HFBII).

functional groups such as hydroxyl ( $\text{-OH}$ ), carbonyl ( $\text{C=O}$ ) and carboxyl ( $\text{COOH}$ ). In addition to these elements, FCBs may contain small amounts of nitrogen and sulfur, depending upon the nature of hydrocarbons used in the manufacture. The characteristic peak of FCBs is due to the C-F stretching in the range of  $1200\text{-}1250\text{ cm}^{-1}$ . The main peaks visible in the spectrum of the HFBII in solution are the Amide I band ( $1600\text{ cm}^{-1}$ ), mainly associated with the  $\text{C=O}$  stretching vibration and Amide II results from the N-H bending vibration and from the C-N stretching

vibration. FT-IR analysis confirmed the simultaneous presence of both HFBII and CBs in the final water dispersion.

### 3.3.3 DLS ANALYSIS OF FLUORINATED CARBON BLACKS IN HFBII-MilliQ WATER

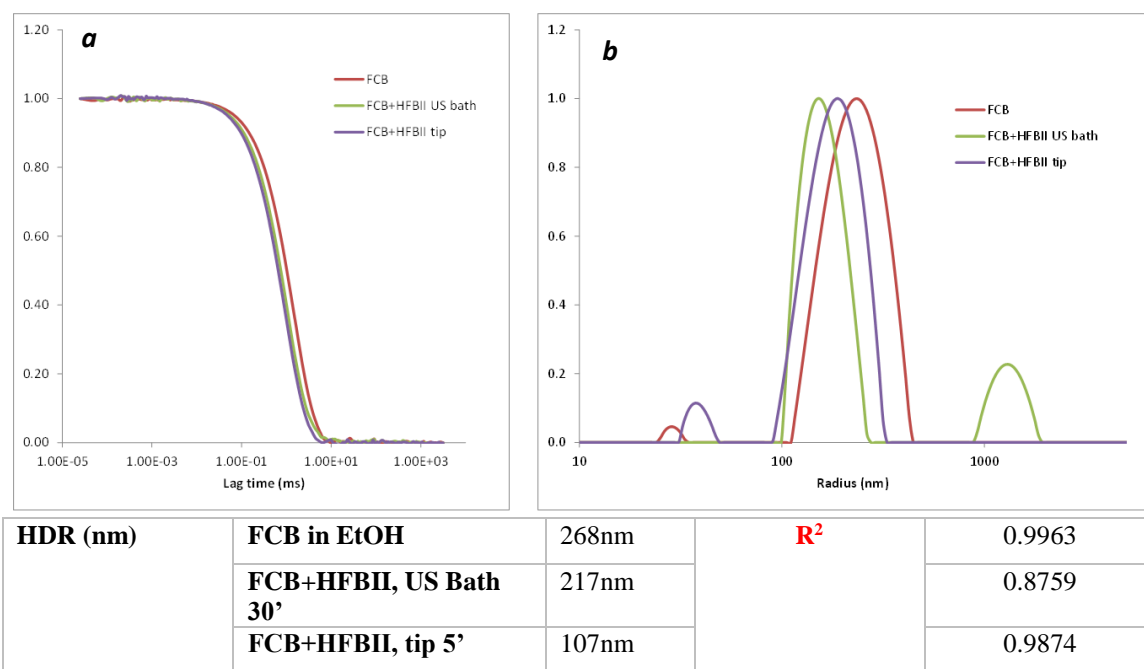


Figure 23. DLS analysis of fluorinated carbon blacks in HFBII-MilliQ: a) Correlation functions at 90° b) Intensity-weighted average size distribution at 90° obtained with CONTIN fit.

Dynamic Light Scattering analysis (DLS) graphs the size distribution of particles in solution. Figure 23a shows that the correlation functions at 90° of FCBs dispersed in organic solvent (red line), FCBs in HFBII-MilliQ dispersed by 30 min US bath (green line), and FCBs in HFBII-MilliQ prepared by 5 min tip sonication (purple line). Figure 23b compares the intensity-weighted average hydrodynamic radius at 90° calculated by CONTIN fit for the same three samples. DLS data show that the starting FCB particles are less polydisperse than the non-fluorinated analogues (CBs). Their coating by HFBII in water have almost no effect on the average size and polydispersity of their aggregates, if compared to their suspension in organic solvent, independently from which dispersion protocol was used (US bath or tip sonication). This observation is in agreement with TEM analyses and with the different stability observed



for the samples. As previously reported for CBs, FCBs in organic solvents sedimented quite fast, whereas their dispersions in an aqueous solution of HFBII were stable for almost 24 hours.

### 3.3.4 $^{19}\text{F}$ -NMR ANALYSIS OF FLUORINATED CARBON BLACKS IN HFBII-MilliQ WATER

$^{19}\text{F}$ -NMR spectra were recorded at 305 K on a Bruker AV400 spectrometer operating at 400 MHz for the  $^{19}\text{F}$  nucleus. The dispersion of FCBs in water and HFBII (400  $\mu\text{L}$ ) was placed in a coaxial NMR tube, with a capillary insert containing 100  $\mu\text{L}$  of deuterated water ( $\text{D}_2\text{O}$ ) for the lock. The capillary contained also 2,2,2-trifluoroethanol (TFE) as reference.

Figure 24 reports the  $^{19}\text{F}$  NMR spectrum of FCBs with HFBII in MilliQ prepared using ultrasound bath and Figure 25 shows the  $^{19}\text{F}$  NMR spectrum of FCBs with HFBII in MilliQ prepared using tip sonicator for 5 minutes.

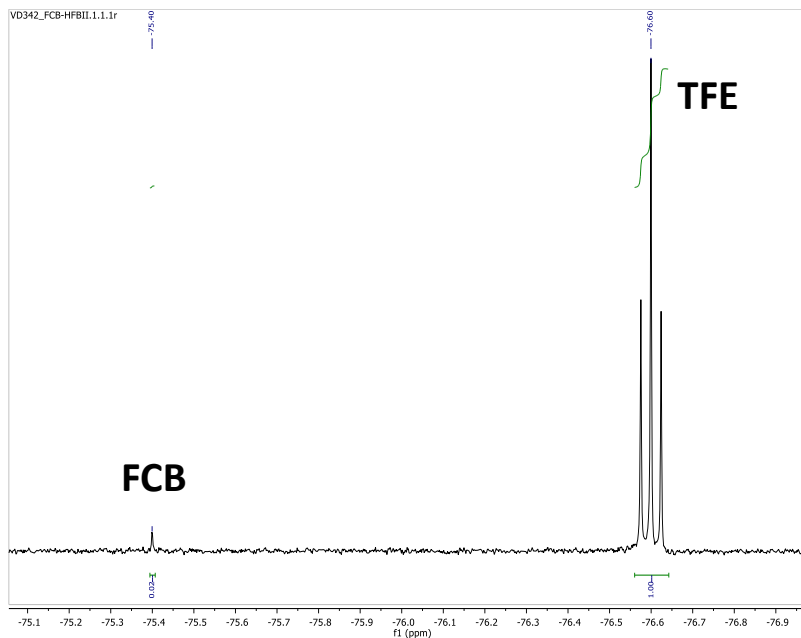


Figure 24  $^{19}\text{F}$ -NMR spectra (ref. 2,2,2-trifluoroethanol in  $\text{D}_2\text{O}$ ) FCB + HFBII – US bath 30'

— — —

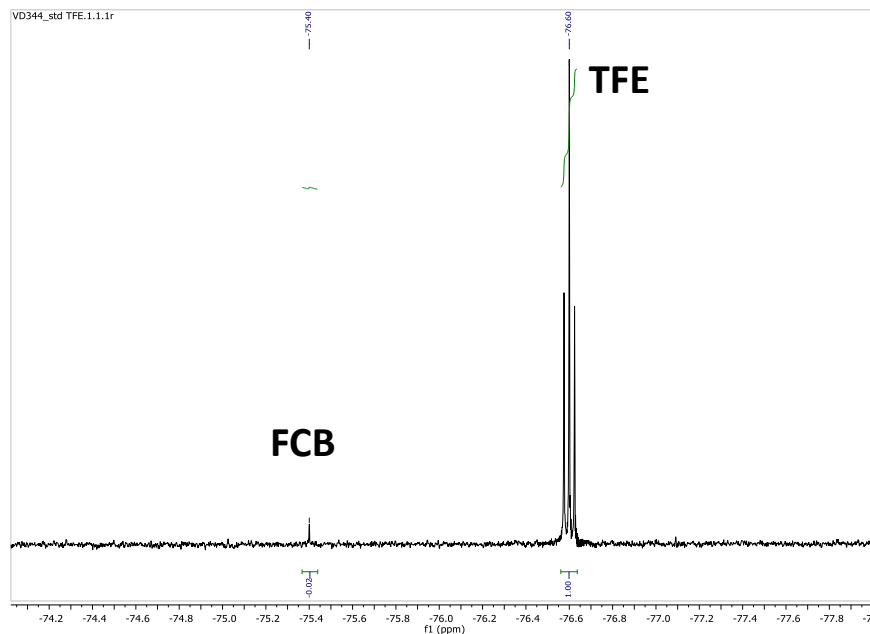


Figure 25  $^{19}\text{F}$ -NMR spectra (ref. 2,2,2-trifluoroethanol in  $\text{D}_2\text{O}$ ) FCB + HFBII – Tip sonicator 5' min

The spectra of both FCB aqueous dispersion showed the signal given by TFE, which is a triplet at a chemical shift of -76.6 ppm, and a singlet signal at -75.4 ppm due to the fluorine atoms present on carbon blacks.

The presence of such signal confirms that FCBs are actually dispersed in the aqueous solution of HFBII, because our  $^{19}\text{F}$  NMR instrument can detect only the resonance of fluorine in solution. Furthermore, the integral ratio between the peak area of FCBs and TFE is the same for both samples, confirming that in the case of fluorinated carbon blacks both sonication techniques gave similar results.

## 4. CONCLUSION AND FUTURE PERSPECTIVES

This thesis project focused on the use of a naturally occurring amphiphilic protein, named Hydrophobin (HFBII), to disperse hydrophobic carbon nanomaterials in water by simple suspension methods such as tip sonication and ultrasound bath treatment. Initially, carbon blacks and fluorinated carbon blacks were dispersed in organic solvents (ethanol or chloroform) for comparison. The resulting dispersions were highly unstable and started to precipitate already after 15-30 minutes. Both CBs and FCBs are not dispersible in water, unless their surface is chemically functionalized with hydrophilic groups, like carboxylate units. The main aim of this thesis was to disperse CBs and FCBs in aqueous media without performing any chemical modification of their surface, exploiting a natural surfactant protein that is known to coat several kinds of hydrophobic materials. Two different protocols were used to achieve this target and were compared to one another. In the first method, the mixture of CBs/FCBs and HFBII in MilliQ water was treated in an ultrasound bath for 30 minutes. The second method consisted in a tip sonication treatment for 5 minutes of the same mixture. All the samples were then characterized and analyzed using DLS, ATR-FTIR,  $^{19}\text{F}$ -NMR and TEM.

Data reported in the results section of this thesis showed that HFBII was able to effectively film CBs and FCBs in water, and gave quite stable aqueous dispersions of their aggregates. Tip sonication improved the stability in time of the resulting dispersions, and generally led to smaller aggregates than ultrasound bath treatment. Hence HFBII proves to be a good surfactant in making stable dispersion of these peculiar carbon nanomaterials, especially in the case of FCBs. These protocols can be further optimized to enhance the dispersion stability, decrease the aggregates' size and polydispersity.

The surprising surface-activity of Hydrophobins has made them alluring competitors in a wide range of surface-engineering applications to date. Hydrophobins as a biosurfactant have a wide range of application in the field of Pharmaceuticals, microfluidics, tissue engineering and green chemistry synthesis. Hydrophobins may be useful as adjuvant in combination with

chemotherapy and radiation or may be even used at the same time to formulate hydrophobic anti-cancer drugs.

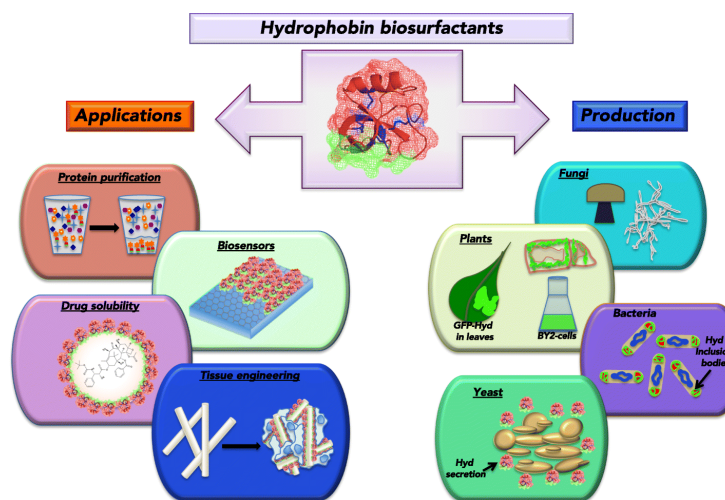


Figure 26. Hydrophobin Prospects in the field of biosurfactants [16].

Furthermore, molecules that allow specific targeting to cancer cells could be introduced via genetic engineering or adsorption. The bioavailability of water-insoluble drugs can be increased by creating nanoparticles via complex methods such as milling and high-pressure homogenization. The particles are stabilized (preventing aggregation) by addition of, e.g., surfactants. Hydrophobins offer a simple and generic alternative to create and stabilize nanoparticles.

Hydrophobins offer a non-covalent alternative for conventional surface modification methods. The latter are complicated, time consuming, and show unstable hydrophilicity. Hydrophobins adsorbed to a substrate can be used to immobilize proteins. Hydrophobins can be used in various applications[36]. The fact that hydrophobins do seem to be neither toxic (they are ingested by humans upon consumption of mushrooms and fungus-fermented foods) nor cytotoxic or immunogenic indicates that they can be safely used in medical and food applications. Hydrophobins all show self-assembly at hydrophilic-hydrophobic interfaces, but the properties of their water-soluble forms and assemblages differ. For instance, solubility and stability of class I and class II hydrophobins differ. Hydrophobins cannot yet be produced in gram per liter

quantities hampering their use in medical and technical applications. However, BASF succeeded to produce the hydrophobins in quantities sufficient for large-scale applications. This brings the potential of hydrophobins in applications in daily life nearby. To get at this objective hydrophobins needs to be analysed thoroughly, complete study with several particles needs to be performed to know the degradability, efficiency of the protein and cytotoxicity.

## 5. REFERENCES

1. Dichiarante, V., Milani, R. and Metrangolo, P. (2018). Natural surfactants towards a more sustainable fluorine chemistry. *Green Chemistry*, 20(1), pp.13-27.
2. Morris, V., Linser, R., Wilde, K., Duff, A., Sunde, M. and Kwan, A. (2012). Solid-State NMR Spectroscopy of Functional Amyloid from a Fungal Hydrophobin: A Well-Ordered  $\beta$ -Sheet Core Amidst Structural Heterogeneity. *Angewandte Chemie International Edition*, 51(50), pp.12621-12625.
3. Bayry, J., Aimanianda, V., Guijarro, J., Sunde, M. and Latgé, J. (2012). Hydrophobins—Unique Fungal Proteins. *PLoS Pathogens*, 8(5), p.e1002700.
4. Linder, M., Szilvay, G., Nakari-Setälä, T. and Penttilä, M. (2005). Hydrophobins: the protein-amphiphiles of filamentous fungi. *FEMS Microbiology Reviews*, 29(5), pp.877-896.
5. Zhang, X., Penfold, J., Thomas, R., Tucker, I., Petkov, J., Bent, J., Cox, A. and Grillo, I. (2011). Self-Assembly of Hydrophobin and Hydrophobin/Surfactant Mixtures in Aqueous Solution. *Langmuir*, 27(17), pp.10514-10522.
6. Milani, R., Monogioudi, E., Baldrighi, M., Cavallo, G., Arima, V., Marra, L., Zizzari, A., Rinaldi, R., Linder, M., Resnati, G. and Metrangolo, P. (2013). Hydrophobin: fluorosurfactant-like properties without fluorine. *Soft Matter*, 9(28), p.6505.
7. Yang, W., Ren, Q., Wu, Y., Morris, V., Rey, A., Braet, F., Kwan, A. and Sunde, M. (2012). Surface functionalization of carbon nanomaterials by self-assembling hydrophobin proteins. *Biopolymers*, 99(1), pp.84-94.
8. Wessels, J., De Vries, O., Asgeirsdottir, S. and Springer, J. (1991). The thn mutation of *Schizophyllum commune*, which suppresses formation of aerial hyphae, affects expression of the Sc3 hydrophobin gene. *Journal of General Microbiology*, 137(10), pp.2439-2445.
9. *Advanced Carbon Materials Michio Inagaki*, in *Handbook of Advanced Ceramics (Second Edition)*, 2013.
10. Dai, H. (2002). Carbon Nanotubes: Synthesis, Integration, and Properties. *Accounts of Chemical Research*, 35(12), pp.1035-1044.
11. Wang, J., Li, M., Shi, Z., Li, N. and Gu, Z. (2002). Direct Electrochemistry of Cytochrome c at a Glassy Carbon Electrode Modified with Single-Wall Carbon Nanotubes. *Analytical Chemistry*, 74(9), pp.1993-1997.
12. Zhao, G., Zhang, L., Wei, X. and Yang, Z. (2003). Myoglobin on multi-walled carbon nanotubes modified electrode: direct electrochemistry and electrocatalysis. *Electrochemistry Communications*, 5(9), pp.825-829.
13. Wösten, H. and de Vocht, M. (2000). Hydrophobins, the fungal coat unravelled. *Biochimica et Biophysica Acta (BBA) - Reviews on Biomembranes*, 1469(2), pp.79-86.
14. Laaksonen, P., Kainlahti, M., Laaksonen, T., Shchepetov, A., Jiang, H., Ahopelto, J. and Linder, M. (2010). Interfacial Engineering by Proteins: Exfoliation and

- Functionalization of Graphene by Hydrophobins. Angewandte Chemie, 122(29), pp.5066-5069.*
15. *A review of current analytical applications employing graphitized carbon blacks, January 2011 Christine M Karbiwnyk Christine M Karbiwnyk K.E. Miller.*
  16. *Berger, B. and Sallada, N. (2019). Hydrophobins: multifunctional biosurfactants for interface engineering. Journal of Biological Engineering, 13(1).*
  17. *Controlled Hybrid Nanostructures through Protein-Mediated Non covalent Functionalization of Carbon Nanotubes\*\* Katri Kurppa,\* Hua Jiang, Gza R. Szilvay, Albert G. Nasibulin, Esko I. Kauppinen, and Markus B. Linder.*
  18. *Schulz, A., Liebeck, B., John, D., Heiss, A., Subkowski, T. and Böker, A. (2011). Protein–mineral hybrid capsules from emulsions stabilized with an amphiphilic protein. Journal of Materials Chemistry, 21(26), p.9731.*
  19. *Yan, Q., Gozin, M., Zhao, F., Cohen, A. and Pang, S. (2016). Highly energetic compositions based on functionalized carbon nanomaterials. Nanoscale, 8(9), pp.4799-4851.*
  20. *Lin, Jing, Xiaoyuan Chen, and Peng Huang. "Graphene-based nanomaterials for bioimaging." Advanced drug delivery reviews (2016).*
  21. *B.J. Berne and R. Pecora. Dynamic light scattering. Dover Publications, Mineola, 2000.*
  22. *Simonescu C. Advanced Aspects of Spectroscopy. Akhyar Farrukh M (ed.). InTech 2012. ISBN: 978-953-51-0715-6*
  23. *Tejedor MI, Anderson MA. In Situ Attenuated Total Reflection Fourier Transform Infrared Studies of the Goethite (α-FeOOH)-Aqueous Solution Interface. Langmuir 1986;2(2):203–210.*
  24. *Harrick NJ. Surface Chemistry from Spectral Analysis of Totally Internally Reflected Radiation. Journal of Physical Chemistry 1960;64(9):1110–1114.*
  25. *Fahrenfort J. Attenuated Total Reflection: A New Principle for the Production of Useful Infrared Reflection Spectra of Organic Compounds. Spectrochimica Acta 1961;17(7):698–709.*
  26. *Simonescu C. Advanced Aspects of Spectroscopy. Akhyar Farrukh M (ed.). InTech 2012. ISBN: 978-953-51-0715-6. Available from : <http://www.intechopen.com/books/advanced-aspects-of-spectroscopy>.*
  27. *F. M. Mirabella, Jr., Practical Spectroscopy Series; Internal reflection spectroscopy: Theory and applications, Marcel Dekker, Inc.; Marcel Dekker, Inc., 1993, 17-52.*
  28. *Tang, C. Y., & Yang, Z. (2017). Transmission Electron Microscopy (TEM). Membrane Characterization, 145–159. doi:10.1016/b978-0-444-63776-5.00008-5*
  29. *Transmission electron microscopy, David B. Williams and C. Barry Carter (Plenum, 1996)*
  30. <http://chem.ch.huji.ac.il/nmr/whatisnmr/quad.html>
  31. *Rose-Sperling, D., Tran, M., Lauth, L., Goretzki, B. and Hellmich, U. (2019). 19F NMR as a versatile tool to study membrane protein structure and dynamics. Biological Chemistry, 0(0).*

32. Li, D., & Sun, G. (2007). *Coloration of textiles with self-dispersible carbon black nanoparticles*. *Dyes and Pigments*,72(2), 144-149. doi:10.1016/j.dyepig.2005.08.011
33. Zhang, W., Dubois, M., Guérin, K., Bonnet, P., Kharbache, H., Masin, F., Hamwi, A. (2009). *Fluorinated nanocarbons using fluorinating agent: Strategies of fluorination and applications*. *The European Physical Journal B*,75(2), 133-139. doi:10.1140/epjb/e2009-00425-7.
34. Thomas, P., Mansot, J. L., Molza, A., Begarin, F., Dubois, M., & Guérin, K. (2014). *Friction Properties of Fluorinated Graphitized Carbon Blacks*. *Tribology Letters*,56(2), 259-271. doi:10.1007/s11249-014-0406-0.
35. Boland, S., Hussain, S., & Baeza-Squiban, A. (2014). *Carbon black and titanium dioxide nanoparticles induce distinct molecular mechanisms of toxicity*. *Wiley Interdisciplinary Reviews: Nanomedicine and Nanobiotechnology*,6(6), 641-652. doi:10.1002/wnan.1302
36. Han A. B. Wösten & Karin Scholtmeijer (December 2014) *Applications of hydrophobins: current state and perspectives* Received: 29 October 2014 /Revised: 8 December 2014 /Accepted: 9 December 2014 Springer-Verlag Berlin Heidelberg 2015